OXFORD UNIVERSITY PRESS | Annals of Botany

ADAPTIVE VALUE OF MARGINAL POPULATIONS: INTEGRATING SELECTIVE SIGNALS, NEUTRAL PROCESSES AND TEMPORAL SCALES

Journal:	*Annals of Botany*
Manuscript ID	AOB-2025-606
Manuscript Type:	Original Article
Date Submitted by the Author:	28-Aug-2025
Complete List of Authors:	Lara-Romero, Carlos; Rey Juan Carlos University (URJC); Universidad Rey Juan Carlos Instituto de Investigacion en Cambio Global Morente-López, Javier ; Goethe University Frankfurt, Department of Plant Evolutionary Ecology Iriondo, Jose; Rey Juan Carlos University (URJC) Garcia - Fernández, Alfredo; Universidad Rey Juan Carlos Instituto de Investigacion en Cambio Global, Biology and Geology, pHysics and Inorganic Chemistry Sacristan - Bajo, Sandra; Universidad Rey Juan Carlos Instituto de Investigacion en Cambio Global, Biology and Geology, Physics and Inorganic Chemistry González-Martínez, Santiago C.; INRAE, UMR1202 BIOGECO: Biodiversité Gènes et Communautés 69 route d'Arcachon F-33610 Cestas, France
Subject Area:	ecological genomics, ecology, evolutionary ecology, evolutionary genomics, abiotic stress, adaptive evolution, SNPs, spatial ecology
Subject Area (free entry):	

Original Article

ADAPTIVE VALUE OF MARGINAL POPULATIONS: INTEGRATING SELECTIVE SIGNALS, NEUTRAL PROCESSES AND TEMPORAL SCALES

Carlos Lara-Romero[1,2*], José M. Iriondo[1,2], Alfredo García-Fernández A[1,2], Javier Morente-López[3], Sandra Sacristán-Bajo[2], Santiago C. González-Martínez[4]

[1]Global Change Research Institute (IICG-URJC), Rey Juan Carlos University (URJC), Madrid, Spain.

[2] Department of Biology and Geology, Physics and Inorganic Chemistry. Rey Juan Carlos University (URJC), Madrid, Spain.

[3]Department of Plant Evolutionary Ecology, Goethe-University Frankfurt, Frankfurt am Main, Germany.

[4]INRAE, Univ. Bordeaux, BIOGECO, Cestas, France.

*Corresponding author: carlos.lara@urjc.es

Running title: ADAPTIVE VALUE OF MARGINAL POPULATIONS

1. ABSTRACT

Background and aims: The importance of populations inhabiting ecologically marginal areas has been extensively debated and shown to depend, to a large extent, on their adaptive value. In the context of climate change, their ecological originality can give marginal populations the capacity to generate unique gene combinations. In this study, we searched for evidence of genetic diversity of adaptive value in marginal populations, through a genomic analysis that encompasses a multidimensional approach, integrating selective signals, neutral processes and temporal scales.

Methods: We used a targeted exome sequencing approach to search for genomic signatures of divergent selection between environmentally marginal and core populations of the Mediterranean alpine species *Silene ciliata*. We also analysed their current genetic population structure and demographic history, as well as signatures of selective sweeps at different levels.

Key results: Populations from core and marginal environments presented similar values of nucleotide diversity, inbreeding, and relatedness. Demographic history played a more relevant role than current environmental conditions in explaining the levels of genetic diversity in marginal populations. We also detected putative signals of diversifying selection among populations inhabiting environmentally marginal and core areas, involving 11 SNPs located in nine genes, as well as five gene pathways.

Conclusions: Populations currently inhabiting marginal environments can diverge from those occupying core areas due to local adaptation despite low overall genetic differentiation. The presence of polymorphisms or traits adapted to specific environments in marginal populations may be particularly valuable in conservation management and restoration, especially in the context of changing environmental conditions.

Key words: climate change, demographic inference, environmental gradients, divergent selection, gene pathways, genetic adaptation.

2. INTRODUCTION

Environmental heterogeneity induces key demographic, genetic and phenotypic differentiation within the natural ranges of species, leading to the identification of *core* and *marginal* areas (Soulé 1973; Pouget *et al.* 2013; Pironon *et al.* 2017). Core areas, characterized by prevalent and, presumably, optimal environmental conditions, host large and, often, genetically diverse populations. In contrast, marginal areas, with atypical and potentially restrictive environmental conditions, present a more complex scenario (Soulé 1973; Brown 1984).

Historically, marginal populations have been perceived as genetically impoverished and maladapted due to genetic drift and inbreeding, thus harbouring little evolutionary potential (Lynch and Gabriel 1987; Lande 1994; Eckert *et al.* 2008a). However, evidence from some species suggests that these populations may be locally adapted to withstand specific environmental pressures. This makes them particularly valuable in the context of climate change, as their genetic diversity may confer adaptive advantages, enhancing the organisms' chances of survival and reproduction (Barrett and Schluter 2008; Morente-López *et al.* 2021). Despite the contrasting views, most studies have been based on limited genetic information, lacking a genomic perspective (Stillman and Amstrong 2015; Razgour *et al.* 2019). Genomic approaches can help to identify unique adaptations in marginal populations as well as to forecast their responses to future environmental pressures (e.g., Theraroz *et al*. 2024).

Genetic adaptation is influenced not only by environmental pressures but also by available genetic diversity, past demographic history and gene flow (Kawecki 2008). High levels of genetic diversity within populations are essential for natural selection and adaptation to take place. Demographic events like bottlenecks can reduce this diversity (Carbognani *et al*. 2019), while population growth can either diminish or augment it,

depending on the influx of new genetic variants (Haghue and Routman 2016). Gene flow can either facilitate adaptation by boosting genetic diversity (Eckert *et al.* 2008b; Morente-López *et al.* 2021; Sacristán-Bajo et al 2025) or hinder it by introducing disadvantageous variants that are removed from the population by natural selection (Lenormand 2002).

When genetic adaptation is studied from a genomic perspective, the genomic signature of selection is superimposed on widespread signatures of the population's demographic history. For instance, both bottlenecks and population growth can generate nucleotide variation patterns that mimic selection (Barton and Etheridge 2004; Ramírez-Soriano *et al.* 2008). Hence, to identify adaptive genetic variants, it is imperative to employ modelling techniques capable of differentiating between the genetic signatures of selection and those stemming from neutral evolutionary processes (e.g., González-Martínez *et al.* 2017; Mayol *et al.* 2020; Evans *et al.* 2023).

Alpine ecosystems exhibit high environmental variability, leading to rapidly shifting selective pressures over short geographical scales (Byars *et al.* 2007; Morente-López *et al.* 2022). In this context, *Silene ciliata* Pourret, a well-studied Mediterranean alpine cushion plant, exemplifies key questions in ecology and evolution in marginal plant populations (García-Fernández *et al.* 2012; Lara-Romero *et al.* 2016; Morente-López *et al.* 2021, 2022). Field studies have shown lower longevity, lower proportion of flowering plants and fewer flowers, fruits, and seeds per plant in the lower-elevation populations (Giménez-Benavides *et al.* 2007; Giménez-Benavides *et al.* 2011). This results in declining growth rates in low-elevation populations, which face local extinction, while higher-elevation populations in more favourable environments show stable growth rates (Giménez-Benavides et al. 2011). In parallel, studies in common-garden conditions, have shown delayed flowering onset, peak and end (Morente-López et al., 2020), lower seed

germination (Giménez-Benavides et al. 2007), and greater drought tolerance (García-Fernández et al., 2013) in low-elevation populations. Interestingly, additional research suggests that populations at lower elevations may possess adaptive advantages over their core counterparts that may be better suited to current and future climatic conditions (Morente-López *et al.* 2020, 2021). Furthermore, in the northern Mediterranean mountain ranges where the species occurs, the last glacial maximum (LGM) have influenced the demographic dynamics and current distributions of many plant species (Feliner 2014; Carbognani *et al*. 2019; Evans *et al*. 2023; Pütz *et al.* 2024), although this aspect has not yet been studied in *S. ciliata*. This lack of knowledge is significant because demographic history could have influenced not only the current distribution of the species, but also the observed patterns of genetic adaptation. Understanding these patterns in mountain populations requires considering both the existence of LGM microrefugia and the dynamics of rear-edge and leading-edge populations (Hampe & Petit 2005; Opgenoorth *et al.* 2009; Vila-Cabrera *et al.* 2019). LGM microrefugia represent localized, climatically stable areas where species persisted during glacial periods, often corresponding to present-day rear-edge populations (Rull 2009). Rear edge populations, located at the oldest and most stable habitat margins, reflect ancestral conditions. In contrast, leading edge populations, found at the most recent and dynamic habitat margins, reflect modern conditions and exhibit rapid adaptations to ongoing environmental changes (Hampe & Petit 2005; Vila-Cabrera *et al.* 2019).

In this study, we aimed to assess the adaptive value of marginal populations through a genomic analysis that encompasses both selective and neutral processes, using a multiscale perspective that considers also recent and ancient processes. Our goal was to explore how past climatic fluctuations—particularly the LGM—and present-day environmental gradients have shaped the patterns of genomic variation in core and

marginal populations. We sequenced 2,414 candidate genes in six natural populations (three core and three marginal), based on previous research that identified SNPs associated with environmental stress responses (Sacristán-Bajo *et al*. 2019). Using F_{ST}-outlier detection to assess long-term adaptation and selective sweep analyses for more recent events, we identified potentially adaptive variation across different timescales. Our analysis of adaptive genetic diversity extended to gene pathways to investigate the role of gene networks in adaptation (Olson-Manning *et al*. 2012; Berg and Coop 2014; Exposito-Alonso *et al*. 2018). In addition, we examined spatial genetic structure and population dynamics using demographic inference models. To date, only a few studies have assessed the adaptive value of marginal populations using combined analyses of population genetic structure, demographic history and genomic signals of selection (e.g., Yang *et al*. 2016; Temunović *et al*. 2020; Yuan *et al*. 2023). Moreover, none has applied a multidimensional framework integrating all these perspectives. In our study, we asked the following questions:

1. Do core and marginal populations differ in levels of genetic diversity, inbreeding or relatedness?
2. What is the spatial genetic structure of the studied populations? Which candidate genes and biological pathways may underlie adaptive genetic differentiation between core and marginal populations?
3. Have there been abrupt changes in effective population sizes over time? If so, can they be linked to the LGM, and are there genomic signatures (e.g., of selective sweeps) indicative of adaptation in either rear-edge or leading-edge contexts?

We hypothesised that distinct selective pressures operating on core versus marginal populations have driven genetic differentiation between them. We further expected that contemporary environmental stressors have accelerated demographic decline in marginal

populations, reducing their genetic diversity. Finally, we expected that the LGM induced a severe demographic contraction, generating a genetic bottleneck signature still detectable in present-day genetic variation.

3. MATERIALS AND METHODS

3.1 Study species and populations

Silene ciliata Pourr. (Caryophyllaceae) is a dwarf cushion perennial plant that inhabits Mediterranean alpine habitats with marked environmental gradients. It has flowering stems that grow up to 15 cm tall, with each stem bearing 1 to 5 flowers. Its fruit capsules contain up to 100 seeds, which are dispersed by wind in August and September. The seeds are small, averaging 0.59 mg in mass and 1.1 to 1.5 mm in diameter, and lack specialized dispersal structures, making the species primarily barochorous. Pollination is carried out by syrphid flies, bumblebees, and moths. The plant is self-compatible, but self-pollination is limited due to significant protandry (see Lara-Romero et al. 2014 and references therein). The distribution of *S. ciliata* comprises the mountain ranges of the Northern Mediterranean area from Spain to Bulgaria (Kyrkou *et al.* 2015), reaching its southernmost limit in the Sistema Central of the Iberian Peninsula (Spain). All *S. ciliata* populations from the Sistema Central are diploid and have the same phylogenetic origin, as shown by chloroplast DNA analysis (Kyrkou *et al.* 2015). In these areas, the species grows from 1,800 to 2,500 m in dry cryophilic pastures above the tree line. This Mediterranean Alpine ecosystem has a pronounced summer drought combined with high solar radiation, which typically selects for plant xerophytic traits.

At the end of the summer of 2013, we collected a minimum of thirty randomly selected plants from six populations located in three sub-mountain ranges of the Sistema Central (Spain): Guadarrama (GDM), Gredos (GRD) and Béjar (BJR) (Figure 1 and Table 1). All sampled plants were separated by at least two meters. The Sistema Central is a southwest-

northeast oriented mountain range of approximately 500 km located in the centre of the Iberian Peninsula. GDM, GRD, and BJR are in the western, central and eastern areas of the Sistema Central, respectively. The six studied populations were located at the high and low elevation margins of the sub-mountain ranges (Figure 1 and Table 1). Within each sub-mountain range, the populations were separated by distances ranging from two to four kilometers. High and low elevation margins represent core (optimal) and marginal environmental conditions, respectively, based on the study of the ecological niche and putative selective pressures for the species (Morente-López *et al.* 2022). According to Morente-López *et al*. (2022), core populations inhabit regions where habitat suitability equals or surpasses the highest 33rd percentile of the distribution of ranked suitability values, estimated using the MaxEnt algorithm. Conversely, the marginal populations are found below the lowest 33rd percentile. In marginal populations, vegetation is dominated by dense shrub cover of *Cytisus oromediterraneus* Rivas Mart. et al. and *Juniperus communis* L. subsp. *alpina* (Suter) Celak. *S. ciliata* is restricted to small, isolated *Festuca curvifolia* Lag. ex Lange pastures, and populations are small, with at most a few hundred individuals. In contrast, core populations are extensive, dominated by *Festuca* fellfields with scarce shrubs, and support many thousands of individuals. Marginal populations are subject to shorter snow cover duration and higher minimum temperatures compared to core populations, reflecting the main climatic gradients relevant to the species (Morente-López *et al.* 2022). Cuttings were obtained from the collected plants, rooted and placed in pots in the Universidad Rey Juan Carlos CULTIVE experimental field (https://urjc-cultive.webnode.es). Resulting plants were grown in common garden conditions before DNA extraction in 2015. Further details on the common garden experiment are provided in Morente-López *et al*. (2020).

3.2 Selection of candidate genes for targeted sequencing

The annotated *Silene latifolia* Poir. and *S. ciliata* transcriptomes (GenBank references: GCA_900095335 and PRJNA528948, respectively; see Sacristán-Bajo *et al*. 2019) were used to design an exome capture experiment based on targeted sequencing. We sequenced a total of 2,414 candidate genes with high-confidence annotations. Candidate genes were selected considering three factors that address specific aspects related to genetic differentiation and adaptation in *S. ciliata*. The first set comprised 576 genes carrying SNPs with unusually high allele frequency differentiation between core and marginal populations (Sacristán-Bajo *et al.* 2019). Briefly, these SNPs were identified in a previous study based on 147,118 SNPs distributed along 12,688 sequences obtained from mRNA libraries of leaf tissue without any prior experimental treatment in common garden conditions. The second set comprised 489 genes annotated with the Gene Ontology term "Flower development" (GO: 0009908) or any of the dependent and more specific terms. These genes are expected to be involved in the development of the flower over time, from its formation to its mature structure. This set of genes was selected because previous quantitative genetic studies in *S. ciliata* indicate the existence of important differences, probably related with contrasted selective pressures, in the flowering phenology of plants from marginal and core populations (Giménez-Benavides, García-Camacho, *et al.* 2011; Morente-López *et al.* 2020). Finally, the third set included 1,349 annotated genes associated with general processes that result in a change in state or activity of a cell or an organism because of an abiotic stimulus (GO: 0009628 or any of the more specific terms). This third set was included in the study to detect a broad range of new candidate genes under divergent selection not previously identified in *S. ciliata*, as previous work on the species was hampered by low statistical power and may have left much of the potential adaptive variants unidentified.

3.3 DNA extraction, targeted sequencing and SNP calling

We used the DNeasy Plant minikit (QIAGEN, Valencia, USA) to extract and isolate DNA from 94 plants (Table 1), 15-17 for each of the six studied populations. Library preparation covering the targeted sequences followed the manufacturer's protocol for Nugen SeqCap Developer kit. Samples were sequenced as 96-plex on a HiSeq2500 lane with paired-reads of 125 bp. Demultiplexing of reads was carried out with CASAVA 1.8.2 (Illumina Inc., San Diego, CA). Reads were masked for adapter contamination with *cutadapt* and low-quality bases were removed using *erne-filter* (ERNE v.1.4.5). Alignment was carried out with BWA MEM v.0.7.10 (https://github.com/lh3/bwa). The aligned sequences obtained from the targeted exome sequencing were deposited in GenBank with accession number PRJNA851086. Prior to SNP calling, alignments were filtered for low mapping quality (<10) and reads were realigned around indels using GATK 3.6 (McKenna *et al.* 2010). SNP calling was performed on the entire sample simultaneously using the *UnifiedGenotyper* implemented in the GATK suite, which allowed the initial identification of ca. 185,000 SNPs.

Raw SNP data were filtered using VCFtools v0.1.14 (Danecek *et al.* 2011) and *vcffilter* function of VCFLIB (Garrison *et al.* 2022). Only biallelic SNPs with fewer than 20% missing data were kept. Indels were also removed from the dataset. SNPs were then filtered following the hard filtering suggested by GATK's user guide (https://gatk.broadinstitute.org/). This stringent filtering reduced the SNP dataset to 112,751 SNPs. Further, SNPs from paralogous genes were filtered combining two approaches. First, the SNP dataset was filtered by Hardy-Weinberg disequilibrium and polymorphism excess (Chen *et al.* 2014). To apply this filter, we estimated F_{IS} in sliding windows of 150 bp with a step of 50 bp. Sliding windows with an average F_{IS} lower than -0.5 were filtered (Hohenlohe *et al.* 2013; McKinney *et al.* 2017), which entailed the

removal of 27,728 SNPs. Second, for the retained dataset (85,023 SNPs), we applied the *HDplot* method. *HDplot* combines information from the relative proportion of heterozygotes in a population (*H*) and the deviation of allele-specific reads of each locus from a 1:1 ratio (*D*), allowing the identification of paralogous loci throughout the range of allele frequencies (McKinney *et al.* 2017). A total of 13,362 SNPs (16%) with *H* greater than 0.65 and $|D| > 20$ were classified as located in paralogous sequence and subsequently removed, resulting in a final SNP dataset of 71,661 SNPs distributed in 2,278 genes.

3.4 Nucleotide diversity, population structure and demographic history

Nucleotide diversity, inbreeding and relatedness

Nucleotide diversity by population (Tajima's π and Watterson's θ) and standard neutrality tests (Tajima's *D*, and Fu & Li's *D** and *F**) were computed using mstatspop (https://github.com/CRAGENOMICA/mstatspop). Additionally, we estimated the number of polymorphic sites, average inbreeding coefficients (*F*) and pairwise relatedness (as evaluated by unadjusted A_{jk} statistic) for each population using VCFtools v0.1.14 (Danecek *et al.* 2011).

Population genetic structure

We investigated population genetic structure using the hierarchical analysis of molecular variance (AMOVA) implemented in Arlequin v3.5.2 (Excoffier and Lischer 2010). The analysis was conducted at three levels: (1) among mountain ranges; (2) between core and marginal populations within mountain ranges; and (3) within populations. Genetic differentiation was calculated for all three hierarchical levels, leading to estimates for F_{CT} (among mountain ranges), F_{SC} (between core and marginal populations within mountain ranges) and F_{ST} (among populations overall). F_{ST} was also calculated between all pairs of

populations, and the significance levels of pairwise F_{ST} estimates were determined by permutation tests (10,000 permutations). Population genetic structure was also inferred by a Bayesian clustering method using fastStructure, with *K* groups from *K*=1 to *K*=6 (the number of localities in our sample), and the simple prior. For improved ancestry estimates and to identify subtle structure, the logistic prior was executed at values of *K* similar to those identified when using the simple prior. Then runs for *K*=2 and *K*=3 (the best *K*) were repeated ten times, and averaged *Q* values (i.e., the individual assignment probability to each of the *K* groups) were used to draw bar plots. As an alternative to AMOVA and fastStructure, we used a Neighbour-net phylogenetic network (NNet) constructed in SplitsTree v 4 (Huson and Bryant 2006), based on uncorrected_p distance with default parameters and 1,000 bootstraps. In order to account for gene flow while inferring the relationships among *S. ciliata* populations, we also used TREEMIX v1.13 (Pickrell and Pritchard 2012). This method models patterns of both population splits and admixtures accessing the covariance structure of allele frequencies between populations and performing a Gaussian approximation for genetic drift, improving the fit of the inferred model by enabling migration edges. TREEMIX analyses were implemented with 500-SNP bootstrap resampling and considering a different number of migration events, ranging from zero to 10.

Demographic inference

Demographic inference at population level: An overall negative Tajima's *D* indicated an excess of low frequency polymorphisms (see Results), suggesting population growth. Based on these results, we tested multiple demographic models for each population separately using the coalescent approach implemented in Fastsimcoal2 v.2.6.0.2 (Excoffier *et al.* 2013). Fastsimcoal2 estimates the composite likelihood of a specific demographic scenario given the observed data as well as population genetic parameters

such as divergence time, effective population size and gene flow, using the site frequency spectrum (SFS) as input. Un-folded site frequency spectra (calculated from observed counts of the derived allele) were generated separately for each of the six populations using VCF2SNPs (Liu *et al.* 2018). To maximize statistical power, we used all SNPs, including those in intragenic regions, for demographic inference, assuming most behave neutrally or quasi-neutrally. This assumption is supported by low levels of linkage disequilibrium (mean $r^2 = 0.11$) and a very small proportion of SNPs showing signatures of selection (see Results). We compared three demographic models (Figure 2). The first "Stationary" model represents a null model consisting in a population of constant size and is defined by a single parameter, the current population size (N_{CUR}). The second "Expansion" model is defined by three parameters: N_{CUR}, a time of instantaneous population size change (T_{EXP}) and a population size prior to T_{EXP}. The third "Bottleneck" model is characterized by four parameters: N_{CUR}, a time at which the bottleneck began (T_{BOT}), a population size during the bottleneck event (N_{BOT}), and a population size prior to T_{BOT} (N_{ANC}). The duration of the bottleneck event was fixed at 100 generations to avoid problems associated with model overparameterization. We performed 100 independent runs for each population and demographic model consisting of 50 cycles of the Brent algorithm and 100,000 simulations. The maximum-likelihood runs under each model were then compared using AIC to select the optimal model for each population. Once the optimal model was identified, we estimated confidence intervals (CIs) by performing 100 parametric bootstraps based on best-model parameters. Mutation rate was estimated from the data assuming a generation time of two years, which reflects the time required for the plant to reach reproductive maturity (Giménez-Benavides *et al.* 2011).

Demographic inference at mountain range level: Previous studies have suggested historical environmental fluctuations related to glaciations affecting *S. ciliata* populations

in central Spain (Morente-López *et al.* 2018). Glacial pulses would have been responsible for shifting *S. ciliata* populations to lower elevations. Postglacial recolonization of higher elevations from lower areas would have originated a front-advancing edge by a subset of the populations at lower elevation. To better understand the potential effect of environmental fluctuations during glaciations on *S. ciliata* populations, we used Fastsimcoal2 to statistically compare the relative fit of multi-population demographic models ("mountain models") incorporating three possible demographic scenarios involving both core and marginal populations (Figure 2b). The first model ("Isolation of two populations") was parametrised with the current population size of marginal (N_M) and core populations (N_O), and a time of instantaneous split (T_{DIV}) from a common ancestral population (N_{ANC}); it represents a simple scenario without effective population size changes. The second model ("Bottleneck and Isolation of two populations") also considered the split of marginal and core populations from a common ancestral population but included a bottleneck event in the ancestral population prior to the split. This bottleneck event was modelled defining a time when the bottleneck began(T_{BOT}), a population size during the bottleneck event (N_{BOT}) and a population size posterior to T_{BOT} (N_{DIV}). Finally, the third model ("Bottleneck and Divergence of a population") considered marginal populations as a result of a bottleneck in the ancestral population from which the core populations would have subsequently diverged; this model reflects the suggested glacial dynamics of the species in the Sistema Central mountain range described above. The three models included migration between marginal and core populations after the divergence event (M_{MC} and M_{CM}), as considering gene flow always improved model fitting (data not shown). The modelling set-up and assessment of model performance was the same as described for the models fitted at the population level.

3.5 Detecting distinct signatures of selection in marginal vs core populations

Hierarchical F_{ST}-outlier analyses

To investigate the contribution of natural selection to genetic adaptation in *S. ciliata,* we combined multiple approaches. First, we searched for signals of divergent selection at the single-locus (SNP) level using hierarchical F_{ST}-outlier analyses implemented in Arlequin and BayeScanHierarchical. For Arlequin, we ran 20,000 simulations under a hierarchical island model with 100 demes per level to establish a null distribution. To control for false positives, we applied a False Discovery Rate (FDR) correction and considered loci with a $1–F_{ST}$ quantile < 0.05 as outliers (Storey et al 2003). BayeScanHierarchical, which extends the standard BayeScan Bayesian likelihood method to hierarchical population structure, was used to identify loci with strong evidence of selection (Foll *et al.* 2014). To ensure adequate statistical power, we set the minimum number of iterations to 10,000, the length of 20 pilot runs to 7,500 iterations, and the burn-in-length to 50,000 iterations. Loci having a *Q*-value (analogue to a FDR) lower than 5% were considered to be under strong selection.

Second, we estimated AFDs (Allele Frequency Differentials) between pairs of core and marginal populations. To reinforce the reliability of our results, we applied a strict criterion, considering a locus as a candidate for selection only if it was identified as an outlier by both hierarchical F_{ST} -outlier analyses and showed consistent AFD patterns across all three pairwise comparisons between core and marginal populations. For the AFD comparisons, the expected number of random significant tests was calculated by multiplying the number of SNPs tested by the probability of AFDs going in the same direction in each comparison by chance (0.5^3), indicating that several thousand SNPs could show consistent AFDs in the same direction by chance. However, combining AFDs

with hierarchical F_{ST}-outlier detection at standard FDR of 0.05 allowed us to increase substantially the confidence in our results (FDR of combined test of 0.00625).

Detection of selective sweeps

To identify recent hard selective sweeps, we employed the SWEEPFINDER algorithm implemented in SweeD v.3.1 (Pavlidis *et al.* 2013). We chose to study hard selective sweeps for their capacity to reveal recent genetic adaptation responding to shifting environmental pressures. This method has the benefit to derive the null hypothesis from the background pattern in the data itself, making it more robust to demographic events such as population growth (Nielsen *et al.* 2005; Pavlidis *et al.* 2013). For each gene, Composite Likelihood Ratios (CLRs) were calculated at 30 equally-spaced positions across the target genomic region. To increase statistical power, all CLR scans were run on unfolded SFS and monomorphic sites were included in the analysis (Pavlidis *et al.* 2013). To further increase power to detect selective sweeps, we only applied the test on 1,758 candidate genes that had 10 SNPs or more, which involved 52,740 SNPs. Significance thresholds for selective sweeps detected in each population were obtained by computing the distribution of CLRs in 100 data sets obtained by coalescence simulations in SFS_CODE (Hernandez 2008). The simulations were based in a demographic scenario of population expansion after a bottleneck, which was the most-likely demographic model in all the studied populations based on Fastsimcoal2 (see Results). To ensure a conservative approach, we only considered selective sweeps with higher likelihood than the maximum obtained in the simulations across all core and marginal populations.

Selection at the gene pathway level

We used a procedure developed in humans (Daub *et al.* 2013, 2017) and tested in plants (Mayol *et al.* 2020), to detect the joint effect of selection in biological pathways. For this

purpose, we used KEGG Automatic Annotation Server to map our 2,278 candidate genes and retained 246 biological pathways that included at least four genes. This threshold was selected to provide sufficient statistical power for subsequent analyses while maintaining a reasonable number of pathways for biological interpretation. While a larger number of genes per pathway would provide greater statistical power, it would also significantly reduce the number of pathways analyzed. We refined this gene-pathway list by removing non-plant pathways (see a similar approach in Mayol *et al*. 2020), resulting in a final selection of 86 known pathways in plants. Then, for the maximum value of the coefficient of selection *alpha* estimated by SweeD and BayeScanHierarchical, we performed a gene set enrichment approach as in Daub *et al*. (2013). For this purpose, we used the POLYSEL pipeline (https://github.com/CMPG/polysel). This pipeline calculates for each statistic the SUMSTAT score (Tintle *et al.* 2009), which is the sum of the values for that statistic of all genes in a given pathway. Then, the pipeline compares SUMSTAT scores, after different bias corrections, to a null normal distribution of 500,000 random sets created using a sequential random sampling method (Ahrens and Dieter 1985), with the same size as the original pathway. As in Daub *et al*. (2013), we reported the gene pathways that showed evidence of having collectively higher gene selection coefficients (Q-value < 0.2), which establishes a probability of finding up to 17 pathways falsely identified as significant by chance alone.

4. RESULTS

4.1 Nucleotide diversity, population structure and demographic history

Nucleotide diversity, inbreeding and relatedness

The comparison between core and marginal populations revealed minimal differences in genetic parameters. Nucleotide diversity, inbreeding and relatedness were similar for

individuals in both environments (Table 2, all Wilcoxon rank tests: $P \geq 0.1$). Most neutrality tests were negative (only CAM had a positive result; Table 2) indicating an excess of rare polymorphisms, which can be interpreted as a demographic signature of population expansion.

Population genetic structure

Three-level hierarchical analysis of molecular variance (AMOVA, Table S1) showed that most of the genetic variation (91.3%) was found within populations, though a significant portion of the variation (6.7%) occurred among mountain ranges. A small (2%) but significant genetic differentiation was detected between core and marginal populations within mountain ranges. Pairwise F_{ST} values were significant for all population pairs and ranged between 0.0155 and 0.1201 (Table S2), being higher for comparisons between mountain ranges (mean ± *SD*: 0.086 ± 0.030, *n*= 12) than within mountain ranges (0.022 ± 0.015, *n*=3). The optimal number of genetic groups in the Bayesian clustering analysis performed using fastStructure was *K*=2, with one group corresponding to Guadarrama and the other group corresponding to Bejar and Gredos (i.e., the westernmost) mountain ranges (Figure 3a). The Neighbour-net network (Nnet) exhibited three well defined groups corresponding with the three mountain ranges studied (Figure 3b). Within each mountain range group, individuals from marginal and core populations were not clearly differentiated. The disposition of the three groups within the network indicated that Gredos and Bejar are more closely connected between them than with Guadarrama. Such a partition is also supported by the TREEMIX graph (Figure 3c), which showed evidence of admixture between populations in Bejar (NEG) and Gredos (CAM), and a clear separation of those in Guadarrama (Figure 3c).

Demographic inference

Population level

For all populations, the model incorporating changes in population size due to bottlenecks and subsequent recent expansion ("Bottleneck" model in Figure 2a) was the most supported based on AIC differences (ΔAIC > 100 for all comparisons). In the highest-likelihood parameter set (Figure 4), estimates of ancestral population size (N_{ANC}) averaged 44,191 (range 27,425-69,097). The bottleneck started in all populations around 4,000–9,500 generations ago, which resulted in a strong reduction of the effective population size (mean N_{BOT} = 169, range 54-403). Current population size (N_{CUR}) had a mean of 329 (range 158-525) and represents an increase of between 30% and 75% over N_{BOT}. A recent population expansion was also supported for all populations except CAM by negative neutrality test values (Figure 4; see above).

Mountain range level

Regarding the models fitted for each mountain range, the "Bottleneck and Isolation of two populations" model (Figure 2b) had the lowest AIC scores (ΔAIC > 1500 for all comparisons). The highest-likelihood parameter set (Figure 5) suggests that ancestral populations suffered a bottleneck around 9,000-18,500 generations ago, which reduced drastically their effective population size. After the bottleneck, ancestral populations recovered up to 65% of their previous effective population size. Populations inhabiting current core and marginal areas within each mountain range subsequently diverged around 2,129–13,800 generations ago. After divergence, core and marginal populations were connected by low (i.e., near zero) and asymmetrical gene flow, with higher gene flow from core to marginal populations (mean M_{CM} = 6.62 E-04 *vs*. mean M_{MC} = 7.59 E-05). Estimates of current population sizes were systematically higher for marginal (mean

N_{CUR} = 4,900, range 2,055-8,195) than for core populations (mean N_{CUR} = 2,324, range 55-6,821). Estimates of N_{CUR} were also notably lower for westernmost mountain ranges (55 and 96 for Bejar and Gredos, respectively) than for eastern Guadarrama mountain range (6,821).

4.2 Detecting signatures of selection in marginal *vs* core populations

SNP and gene region level

The hierarchical island model in Arlequin identified 750 SNPs as significant F_{ST} outliers ($P < 0.05$ after FDR correction). Out of them, 35 SNPs showed consistent AFDs in all comparisons between pairs of core and marginal populations. Candidate SNPs belonged to 13 different genes. BayeScanHierarchical detected 170 outlier SNPs and 13 of these (belonging to 11 genes) showed consistent AFDs. Eleven SNPs located on nine genes were outliers using both methods (Table 3), and we considered them as potential candidate loci under divergent selection. These potentially adaptive SNPs/genes are involved in regulation of flower development, oxidation-reduction processes, response to light stimulus, UV protection and different stress responses (Table 3). Out of the nine genes, four were among those associated with adaptation to elevation in previous studies (Sacristán-Bajo *et al.* 2019), four were annotated as GO: 0009628 (response to abiotic stimulus) and two as GO: 0009908 (flower development) (Table 3).

Overall, composite likelihood ratio tests (CLRTs) found slightly more selective sweeps in core populations (mean = 1,303, range 698-2,478) than in marginal ones (mean = 1,186, range 559-2,346). Eighteen selective sweeps located in 10 genes were found in all the populations of the same type (Table 4) and were thus considered as potential candidate gene regions under selection in either marginal or core environments. From them, nine of the 10 genes were found in core populations and only one gene was systematically found in all marginal populations. Only three selective sweeps located in the same gene

(PARG1, coding for a poly(ADP-ribose) glycohydrolase) were found in all the studied populations (Table 4). None of the genes with signs of a selective sweep experienced divergent selection according to F_{ST}-outlier analyses (Tables 3 and 4). Five and four of them were involved in different biological processes associated with responses to abiotic stimulus (GO: 0009628) and flower development (GO: 0009908), respectively, and three were among the candidate genes associated with adaptation to elevation in previous studies (Sacristán-Bajo *et al.* 2019; Table 4).

Gene pathway level

A total of 1,623 out of 2,250 genes mapped on existing KEGG pathway maps for plants (Table S3). Mapped genes were distributed on 86 distinct pathways (Table S3). Five pathways, involving 47 candidate genes, were enriched for positive values of *alpha* estimated by BayeScanHierarchical (Q-value < 0.2; Table 4, Table S3) indicating diversifying selection between core and marginal populations. A low proportion of candidate gene pathways shared genes, with 42 out of the 47 genes being specific to only one of the five pathways. None of these genes were among those found significant in analyses at single-gene level (considering both F_{ST} outliers and selective sweeps; Tables 3 and 4, respectively). Enrichment analysis using the maximum value of *alpha* estimated by SweeD did not detect any biological pathways with significant SUMSTAT scores.

5. DISCUSSION

Remarkably, we found low genetic differentiation between core and marginal populations of *S. ciliata*, suggesting that both environments harbour a wealth of genetic variation on which selection could act. The similar levels of genetic diversity observed may reflect the complex demographic history of the species, including range shifts, expansions, and contractions associated with climatic oscillations during and following the LGM. These

historical processes likely shaped the current distribution of genetic diversity in *S. ciliata*, enabling both core and marginal populations to retain adaptive potential. This challenges the conventional view that marginal populations are genetically impoverished and stresses their role in future responses to environmental challenges (Morente-López *et al.* 2021, 2022).

Based on current declining growth rates, we hypothesized that *S. ciliata* populations inhabiting marginal areas might be genetically impoverished and lack adaptive value (Lynch and Gabriel 1987; Lande 1994; Eckert *et al.* 2008a). Instead, our study revealed an unexpected homogeneity in nucleotide diversity, inbreeding, and relatedness across populations, irrespective of their environmental conditions. Moreover, populations in marginal environments exhibit larger current population size (N_{CUR}), as estimated by historical demography models. This similarity in genetic parameters challenges preconceptions: rather than being genetically deprived, marginal populations possess genetic diversity comparable to their core counterparts. Genetically-based phenotypic differentiation between core and marginal populations, as previously documented (García-Fernández *et al*. 2012; Morente-López *et al*. 2020, 2022; Prieto-Benítez *et al*. 2021), together with the presence of genomic adaptive divergence in marginal populations (see Results), emphasize the adaptive value of *S. ciliata* marginal populations. While these marginal populations retain adaptive genetic diversity, climate change heavily impacts their survival. Environmental conditions at low elevations are constraining the viability of the populations, as evidenced by present-time demographic studies showing declining growth rates and higher local extinction risks at low elevations compared to the stable growth rates in higher elevations (Giménez-Benavides *et al*. 2011; Lara-Romero *et al*. 2014, 2016). Although available adaptive genetic diversity seems not to be enough to adapt to their changing environment, it still may facilitate the adaptation

of higher-elevation populations through adaptive gene flow, as shown in empirical studies (Morente-López *et al*. 2021; Prieto-Benítez *et al*. 2021).

Demographic inferences support a bottleneck around the last glacial maximum and subsequent divergence of populations in core and marginal environments. This divergence is plausible even at small spatial scales, given the species' limited dispersal capacity (Lara-Romero et al. 2014) and the potential for genetic isolation in heterogeneous landscapes, even despite spatial proximity (Budde et al. 2024). While some populations descended to lower elevations, others likely persisted on mountaintops in climatically stable microrefugia (Feliner 2014; Thompson 2020; Pütz *et al*. 2024). These mountaintop populations, consistent with the concept of rear-edge populations (Hampe and Petit 2005; Opgenoorth et al 2009), show lower historical population size (N_{ANC}), marked genetic divergence from marginal populations (as reflected by significant F_{SC}), and a higher number of selective sweeps. These genomic signatures suggest long-term persistence and multiple episodes of positive selection in isolated and stable microrefugia (Colonna *et al*. 2014; Carbognani *et al* 2019; Deng *et al*. 2021).

In contrast, our results suggest that marginal low-elevation populations experienced past expansions during more favourable climatic periods, consistent with the leading-edge dynamics of colonisation into newly suitable environments (Hampe & Petit, 2005). However, progressive warming over the last century has displaced the species' climatic optimum upslope (Giménez-Benavides *et al.* 2007; Morente-López et al 2022), leading to current demographic declines in these now trailing-edge populations (Giménez-Benavides *et al*. 2007; Lara-Romero *et al*. 2014; Morente-López *et al*. 2022). Despite this, their adaptive genetic diversity may still contribute to the evolutionary potential of core populations through adaptive gene flow (Morente-López et al 2021; Prieto-Benítez et al 2022). These findings question typical assumptions about a direct relationship

between genetic diversity, range limits and current environmental suitability, highlighting instead the influence of past demographic history in shaping present-day genetic patterns (Duncan *et al.* 2015; Pironon *et al.* 2015; Yang *et al.* 2016).

The macroevolutionary forces shaping the distribution and diversity of *S. ciliata* have also influenced microevolutionary processes, such as selection on specific genes and pathways. With respect to individual genes, we detected signals of selection in four genes related with flower development (*APS1, NUA, CYP71B37, atg4*). Previous work at the phenotypic level suggested local adaptation for phenological traits in association with elevation (Giménez-Benavides, García-Camacho, *et al.* 2011; Morente-López *et al.* 2020). This is an expected result since in alpine ecosystems flowering phenology is a crucial demographic event (Molau *et al.* 2005; Sedlacek *et al.* 2015), forcing plants to have a fine phenological adjustment to the climate (Scheepens and Sto 2013). Moreover, we also identified candidate genes relevant for abiotic stress response in our study (Table 2). These include *PSBO* and *SCPL49*, recognized as drought-stress response genes (Ashburner and The Gene Ontology Consortium 2000; Berardini *et al.* 2015; Shaar-moshe *et al.* 2015), or *GH3*, which controls hypocotyl elongation, a molecular mechanism critical for germination and seedling establishment (Berardini *et al.* 2015).

Beyond the level of individual genes, our analysis revealed that adaptation in *S. ciliata* involves complex genetic mechanisms, including selection acting on five metabolic pathways. Four of them were involved in essential metabolic functions that are critical for plant survival, namely thiamine, purine, sulfur and seleno compound metabolisms. Abiotic stress alters plant metabolism, inducing biochemical and physiological responses that create tolerance (reviewed in Ramakrishna and Gill 2019). These metabolic adjustments involve fine regulations of several metabolic pathways including those identified here (Lawlor and Cornic 2002; Yan *et al.* 2014; Heinemann and Hildebrandt

2021). The other gene pathway was related to RNA transport from the nucleus to the cytoplasm, which plays pivotal roles in regulation of gene expression. Several studies support the important role that mRNA export mechanisms play in abiotic stress responses of plants (Chinnusamy *et al.* 2008; Ehrnsberger *et al.* 2019; Yeap *et al.* 2019). The detection of this signal at the pathway level suggests that adaptation in species with complex evolutionary histories may involve genetic traits controlled by multiple genes within specific pathways. This challenges the traditional view of adaptation as being driven by single-gene mutations. Remarkably, approaches focused on single loci failed to detect signatures of selection for any of the genes involved in these pathways. Because of their small effect-sizes, genes under "soft" selection are hard to detect by single-locus approaches, although together they can have a large impact on a biological pathway (Olson-Manning *et al.* 2012; Berg and Coop 2014).

The candidate genes and pathways identified in this study offer an initial understanding of the molecular mechanisms underlying the adaptive responses to marginal and core environments. However, it is crucial to consider the possibility of false positives. Notably, certain candidate genes revealed multiple significant SNPs, with some of these genes also previously suggested as potentially involved in adaptation in an RNAseq experiment (Sacristan *et al.* 2019). In addition, our strategy was guided by a focus on adaptive molecular signals concurrently identified in the three replicated elevation gradients, aiming at minimizing the occurrence of false positives (Thornton and Jensen 2007). Nevertheless, further confirmation is necessary to ascertain the adaptive nature of candidate genes and pathways, requiring additional research to establish a clear link between allelic variation and fitness (e.g., Jaramillo-Correa *et al.* 2015; Vangestel *et al.* 2018.

Conclusions

Our findings rejected the hypothesis that marginal populations of *S. ciliata* are genetically impoverished. Instead, they revealed similar levels of genetic diversity in both core and marginal populations, shaped by historical events, with standing genetic variation in marginal populations being essential for adaptation to ongoing climate change. By employing a genomic analysis that encompassed both selective and neutral processes, and adopting a multiscale perspective that considered both recent and ancient dynamics, we provided evidence of past selection in both environments and identified genes potentially associated with flower development and abiotic stress responses. Notably, genetic variation in *S. ciliata* may have partly resulted from selection acting on key metabolic pathways, which highlighted complex mechanisms of adaptation. Further research is needed to validate the adaptive role and fitness effects of these genes, as well as to assess the potential of *S. ciliata* populations to respond to future environmental pressures.

6. FUNDING

This work was supported by projects AdAptA (CGL2012-33528) of the Spanish Ministry of Economy and Competitiveness (MINECO). CLR was supported by a "Juan de la Cierva Incorporación" post-doctoral fellowship (Spanish Ministry of Science: IJC2019-041342-I), by the José Castillejo Mobility Programme for Young Doctors (Spanish Ministry of Science, Innovation and Universities, CAS18/00189) and by a Mobility Grant of COTE Cluster of Excellence granted by Université de Bordeaux. SSB was supported by a FPI pre-doctoral fellowship (MINECO: BES-2017-082317).

7. ACKNOWLEDGEMENTS

Niklaus Zemp from the ETH Zurich Genetic Diversity Centre for providing access to the reference transcriptome of *Silene latifolia*. Alex Widmer from ETH Zurich for his contribution to the design of the experiment. Samples were sequenced by IGA Technology Services (http://www.igatechnology.com).

8. AUTHOR CONTRIBUTIONS

CLR, JML, AGF and JMI designed the experimental study, conducted the fieldwork, and collected the samples. JML with the help of CLR, AGF and JMI performed common garden experiments. CLR, SSB and AGF performed the DNA extractions in the laboratory. CLR and SGM analysed data with the help of SSB and AGF. CLR, SGM and JMI wrote the paper. All authors reviewed the paper and approved the final manuscript.

9. CONFLICT OF INTEREST

All authors declare that they have no conflicts of interest.

10. AI ASSISTANCE ACKNOWLEDGEMENT

The grammar and wording were refined using artificial intelligence with Microsoft Copilot, which was accessed under the institutional license provided by Universidad Rey Juan Carlos.

11. LITERATURE CITED

Ahrens JH, Dieter U. **1985**. Sequential random sampling. *ACM Transactions on Mathematical Software (TOMS)* **11**: 157–169.

Ashburner M, The Gene Ontology Consortium. **2000**. Gene Ontology : tool for the. *Nature Genetics* **25**: 25–29.

Barrett RDH, Schluter D. **2008**. Adaptation from standing genetic variation. *Trends in Ecology and Evolution* **23**: 38–44.

Barton NH, Etheridge AM. **2004**. The Effect of Selection on Genealogies. *Genetics* **166**: 1115–1131.

Berardini TZ, Reiser L, Li D, *et al.* 2015. The Arabidopsis Information Resource : Making and Mining the " Gold Standard " Annotated Reference Plant Genome. *Genesis* **53**: 474–485.

Berg JJ, Coop G. 2014. A Population Genetic Signal of Polygenic Adaptation. *PLoS Genetics* **10**: e1004412.

Brown J. 1984. On the relationship between abundance and distribution of species. *The American Naturalist* **124**: 255–279.

Byars SG, Papst W, Hoffmann AA. 2007. Local adaptation and cogradient selection in the alpine plant, *Poa hiemata*, along a narrow altitudinal gradient. *Evolution* **61**: 2925–2941.

Budde KB, Rellstab C, Heuertz M, Gugerli F, Hanika T, Verdú M, Pausas JG, González-Martínez, S. C. 2024. Divergent selection in a Mediterranean pine on local spatial scales. *Journal of Ecology*, **112**, 278-290.

Carbognani M, Piotti A, Leonardi S, Pasini L, Spanu I, Vendramin GG, Tomaselli M, Petragliad A. 2019. Reproductive and genetic consequences of extreme isolation in *Salix herbacea* L. at the rear edge of its distribution. *Annals of Botany* **124**: 849-860.

Chen N, Van Hout CV, Gottipati S, Clark AG. 2014. Using mendelian inheritance to improve high-throughput SNP discovery. *Genetics* **198**: 847–857.

Chinnusamy V, Gong Z, Zhu J. 2008. Nuclear RNA export and its importance in abiotic stress responses of plants. *Current Topics in Microbiology and Immunology*: 235–255.

Colonna V, Ayub Q, Chen Y, *et al.* 2014. Human genomic regions with exceptionally high levels of population differentiation identified from 911 whole-genome sequences. *Genome Biology* **15**: 1–14.

Danecek P, Auton A, Abecasis G, *et al.* 2011. The variant call format and VCFtools. *Bioinformatics* **27**: 2156–2158.

Daub JT, Hofer T, Cutivet E, *et al.* 2013. Evidence for polygenic adaptation to pathogens in the human genome. *Molecular Biology and Evolution* **30**: 1544–1558.

Daub JT, Moretti S, Davydov II, Excoffier L, Robinson-Rechavi M. 2017. Detection of pathways affected by positive selection in primate lineages ancestral to humans. *Molecular Biology and Evolution* **34**: 1391–1402.

Deng J, Assandri G, Chauhan P, *et al.* 2021. Wolbachia - driven selective sweep in a range expanding insect species. *BMC Ecology and Evolution* **21**: 181.

Duncan SI, Crespi EJ, Mattheus N, Rissler L. 2015. History matters more when explaining genetic diversity within the context of the core–periphery hypothesis SARAH. *Molecular Ecology* **24**: 4323–4336.

Eckert CG, Samis KE, Lougheed SC. 2008a. Genetic variation across species' geographical ranges: The central-marginal hypothesis and beyond. *Molecular Ecology* **17**: 1170–1188.

Eckert CG, Samis KE, Lougheed SC. 2008b. Genetic variation across species' geographical ranges: The central-marginal hypothesis and beyond. *Molecular Ecology* **17**: 1170–1188.

Ehrnsberger HF, Grasser M, Grasser KD. 2019. Nucleocytosolic mRNA transport in plants: Export factors and their influence on growth and development. *Journal of Experimental Botany* **70**: 3757–3763.

Evans A, de Kort H, Brys R, Duffy KJ, Jersáková J, Kull T, Selosse MA, Tsiftsis S, Minasiewicz J, Jacquemyn H. 2023. Historical biogeography and local adaptation explain population genetic structure in a widespread terrestrial orchid. *Annals of Botany* 131: 623–634.

Excoffier L, Dupanloup I, Huerta-Sánchez E, Sousa VC, Foll M. 2013. Robust Demographic Inference from Genomic and SNP Data. *PLoS Genetics* **9**.

Excoffier L, Lischer HEL. 2010. Arlequin suite ver 3.5: A new series of programs to perform population genetics analyses under Linux and Windows. *Molecular Ecology Resources* **10**: 564–567.

Exposito-Alonso M, Vasseur F, Ding W, Wang G, Burbano HA, Weigel D. 2018. Genomic basis and evolutionary potential for extreme drought adaptation in Arabidopsis thaliana. *Nature Ecology and Evolution* **2**: 352–358.

Feliner GN. 2014. Patterns and processes in plant phylogeography in the Mediterranean Basin. A review. *Perspectives in Plant Ecology , Evolution and Systematics* **16**: 265–278.

Foll M, Gaggiotti OE, Daub JT, Vatsiou A, Excoffier L. 2014. Widespread signals of convergent adaptation to high altitude in Asia and America. *American Journal of Human Genetics* **95**: 394–407.

García-Fernández A, Iriondo JM, Escudero A. 2012. Inbreeding at the edge: Does inbreeding depression increase under more stressful conditions? *Oikos* **121**: 1435–1445.

García-Fernandez A, Iriondo JM, Bartels D, Escudero A. 2013. Response to artificial drying until drought-induced death in different elevation populations of a high-mountain plant. Plant Biology 15:93-100.

Garrison E, Kronenberg ZN, Dawson ET, Pedersen BS, Prins P. 2022. A spectrum of free software tools for processing the VCF variant call format: vcflib, bio-vcf, cyvcf2, hts-nim and slivar. *Plos Computational Biology 18*: e1009123.

Giménez-Benavides L, Albert MJ, Iriondo JM, Escudero A. 2011. Demographic processes of upward range contraction in a long-lived Mediterranean high mountain plant. *Ecography* **34**: 85–93.

Giménez-Benavides L, Escudero A, Iriondo JM. 2007. Reproductive limits of a late-flowering high-mountain Mediterranean plant along an elevational climate gradient. *New Phytologist* **173**: 367–382.

González-Martínez SC, Ridout K, Pannell JR. 2017. Range Expansion Compromises Adaptive Evolution in an Outcrossing Plant. *Current Biology* **27**: 2544-2551.e4.

Haghue M, Routman E. **2016**. Does population size affect genetic diversity? A gest with simpatric lizard species. *Heredity* **116**: 92-98.

Hampe A, Petit RJ. 2005. Conserving biodiversity under climate change: the rear edge matters. *Ecology letters*, **8:** 461-467.

Heinemann B, Hildebrandt TM. **2021**. The role of amino acid metabolism in signaling and metabolic adaptation to stress-induced energy deficiency in plants. *Journal of Experimental Botany* **72**: 4634–4645.

Hernandez RD. **2008**. A flexible forward simulator for populations subject to selection and demography. *Bioinformatics* **24**: 2786–2787.

Hohenlohe PA, Day MD, Amish, SJ, Miller, MR, Kamps-Hughes N, Boyer MC, ... & **Luikart, G**. **2013**. Genomic patterns of introgression in rainbow and westslope cutthroat trout illuminated by overlapping paired-end RAD sequencing. *Molecular ecology **22***: 3002-3013.

Huson DH, Bryant D. **2006**. Application of phylogenetic networks in evolutionary studies. *Molecular Biology and Evolution* **23**: 254–267.

Jaramillo-Correa JP, Rodríguez-Quilón I, Grivet D, *et al.* 2015. Molecular proxies for climate maladaptation in a long-lived tree (*Pinus pinaster* Aiton, Pinaceae). *Genetics* **199**: 793–807.

Kawecki T. **2008**. Adaptation to marginal habitats. *Annual Review of Ecology, Evolution, and Systematics* **39**: 321–342.

Kyrkou I, Iriondo JM, García-Fernández A. **2015**. A glacial survivor of the alpine Mediterranean region: Phylogenetic and phylogeographic insights into *Silene ciliata* Pourr. (Caryophyllaceae). *PeerJ* **2015**: 1–19.

Lande R. **1994**. Risk of population extinction from fixation of new deleterious mutations. *Evolution* **48**: 1460–1469.

Lara-Romero C, García-Fernández A, Robledo-Arnuncio JJ, *et al.* 2016. Individual spatial aggregation correlates with between-population variation in fine-scale genetic structure of *Silene ciliata* (Caryophyllaceae). *Heredity* **116**: 417–423.

Lara-Romero C, Robledo-Arnuncio JJ, García-Fernández A, Iriondo JM. **2014**. Assessing intraspecific variation in effective dispersal along an altitudinal gradient: A test in two Mediterranean high-mountain plants. *PLoS ONE* **9**.

Lawlor DW, Cornic G. **2002**. Photosynthetic carbon assimilation and associated metabolism in relation to water deficits in higher plants. *Plant, Cell and Environment* **25**: 275–294.

Lenormand T. **2002**. Gene flow and the limits to natural selection. *Trends in Ecology and Evolution* **17**: 183–189.

Liu S, Ferchaud AL, Grønkjær P, Nygaard R, Hansen MM. **2018**. Genomic parallelism and lack thereof in contrasting systems of three-spined sticklebacks. *Molecular Ecology* **27**: 4725–4743.

López-Moreno JI, Vicente-Serrano SM, Lanjeri S. 2007. Mapping snowpack distribution over large areas using GIS and interpolation techniques. *Climate Research*, **33**: 257.

Lynch M, Gabriel W. **1987**. Environmental Tolerance. *The American Naturalist* **129**: 283–303.

Mayol M, Riba M, Cavers S, *et al.* 2020. A multiscale approach to detect selection in nonmodel tree species: Widespread adaptation despite population decline in Taxus baccata L. *Evolutionary Applications* **13**: 143–160.

McKenna A, Hanna M, Banks E, *et al.* 2010. The Genome Analysis Toolkit: A MapReduce framework for analyzing next-generation DNA sequencing data. *Genome Research* **20**: 1297–1303.

McKinney GJ, Waples RK, Seeb LW, Seeb JE. **2017**. Paralogs are revealed by proportion of heterozygotes and deviations in read ratios in genotyping-by-sequencing data from natural populations. *Molecular Ecology Resources* **17**: 656–669.

Molau U, Nordenhall U, Eriksen B. **2005**. Onset of flowering and climate variability in an alpine landscape: A 10-year study from Swedish Lapland. *American Journal of Botany* **9**: 422–431.

Morente-López J, García C, Lara-Romero C, García-Fernández A, Draper D, Iriondo JM. **2018**. Geography and Environment Shape Landscape Genetics of Mediterranean Alpine Species Silene ciliata Poiret. (Caryophyllaceae). *Frontiers in Plant Science* **9**: 1–15.

Morente-López J, Kass J, Lara-Romero C, Serra-Diaz JM, Soto-Correa JC, Anderson RP, Iriondo JM. 2022. Linking ecological niche models and common garden experiments to predict phenotypic differentiation in stressful environments: Assessing the adaptive value of marginal populations in an alpine plant. *Global Change Biology* **28**: 4143-4162.

Morente-López J, Lara-Romero C, García-Fernández A, Rubio Teso ML, Prieto-Benítez S, Iriondo JM. **2021**. Gene flow effects on populations inhabiting marginal areas: Origin matters. *Journal of Ecology* **109**: 139–153.

Morente-López J, Scheepens JF, Lara-Romero C, Ruiz-Checa R, Tabarés P, Iriondo JM. **2020**. Past selection shaped phenological differentiation among populations at contrasting elevations in a Mediterranean alpine plant. *Environmental and Experimental Botany* **170**: 103894.

Nielsen R, Williamson S, Kim Y, Hubisz MJ, Clark AG, Bustamante C. **2005**. Genomic scans for selective sweeps using SNP data. *Genome Research* **15**: 1566–1575.

Olson-Manning CF, Wagner MR, Mitchell-Olds T. **2012**. Adaptive evolution: Evaluating empirical support for theoretical predictions. *Nature Reviews Genetics* **13**: 867–877.

Opgenoorth L, Vendramin GG, Mao K, Miehe G, Miehe S, Liepelt S, Liu J, Ziegenhagen B. 2010. Tree endurance on the Tibetan Plateau marks the world's highest known tree line of the Last Glacial Maximum. *New Phytologist*, *185*: 332-342.

Pavlidis P, Živković D, Stamatakis A, Alachiotis N. **2013**. SweeD: Likelihood-based detection of selective sweeps in thousands of genomes. *Molecular Biology and Evolution* **30**: 2224–2234.

Pickrell JK, Pritchard JK. **2012**. Inference of Population Splits and Mixtures from Genome-Wide Allele Frequency Data. *PLoS Genetics* **8**: e1002967.

Pironon S, Papuga G, Villellas J, Angert AL, García MB, Thompson JD. **2017**. Geographic variation in genetic and demographic performance: new insights from an old biogeographical paradigm. *Biological Reviews* **92**: 1877–1909.

Pironon S, Villellas J, Morris WF, Doak DF, García MB. **2015**. Do geographic , climatic or historical ranges differentiate the performance of central versus peripheral populations ? *Global Ecology and Biogeography* **24**: 611–620.

Pouget M, Youssef S, Migliore J, Juin M, Médail F, Baumel A. **2013**. Phylogeography sheds light on the central-marginal hypothesis in a Mediterranean narrow endemic plant. *Annals of Botany* **112**: 1409–1420.

Prieto-Benítez S, Morente-López J, Rubio Teso ML, *et al.* 2021. Evaluating Assisted Gene Flow in Marginal Populations of a High Mountain Species. *Frontiers in Ecology and Evolution* **9**: 1–12.

Pütz J, Jansen S, Reutimann O, Rellstab C, Bordács S, Neophytou C. 2024. The influence of post-glacial migration and hybridization on the gene pool of marginal *Quercus pubescens* populations in Central Europe, *Annals of Botany*, mcae216.

Ramakrishna A, Gill S. **2019**. *Metabolic Adaptations in Plants During Abiotic Stress*. Boca Ratón: CRC Press.

Ramírez-Soriano A, Ramos-Onsins SE, Rozas J, Calafell F, Navarro A. **2008**. Statistical power analysis of neutrality tests under demographic expansions, contractions and bottlenecks with recombination. *Genetics* **179**: 555–567.

Razgour O, Forester B, Taggart JB, Bekaer, M, Juste J, Ibáñez C, Puechmaille Sj, Novella-Fernandez, RN, Alberdi A, Manel, S. 2019. Considering adaptive genetic variation in climate change vulnerability assessment reduces species range loss projections. *Proceedings of the National Academy of Sciences*, ***116***:10418-10423.

Rull V. 2009. Microrefugia**.** *Journal of Biogeography* **36**: 481-484.

Sacristán-Bajo S, García-Fernández A, Iriondo JM, Lara-Romero C. **2019**. Transcriptome assembly and polymorphism detection in *Silene ciliata* (Caryophyllaceae). *Plant Genetic Resources: Characterisation and Utilisation* **17**: 452–455.

Sacristán-Bajo S, Lara-Romero C, García-Fernández A, Prieto-Benítez S, Morente-López J, Rubio Teso ML, Torres E, Iriondo JM,. 2019. Assisted gene flow

management to climate change in the annual legume *Lupinus angustifolius* L.: from phenotype to genotype. *Evolutionary Applications* **18**: e70087.

Scheepens JF, Sto J. **2013**. Flowering phenology and reproductive fitness along a mountain slope : maladaptive responses to transplantation to a warmer climate in *Campanula thyrsoides*. *Oecologia* **171**: 679–691.

Sedlacek J, Wheeler JA, Cortés AJ, Bossdorf O. **2015**. The Response of the Alpine Dwarf Shrub *Salix herbacea* to Altered Snowmelt Timing : Lessons from a Multi-Site Transplant Experiment. *PLoS ONE* **10**: e0122395.

Shaar-moshe L, Hübner S, Peleg Z. **2015**. Identification of conserved drought-adaptive genes using a cross-species meta-analysis approach. *BMC Plant Biology* **15**: 111.

Soulé M. **1973**. The epistasis cycle: a theory of marginal populations. *Annual review of ecology and systematics* **4**: 165–187.

Stillman Jh, Armstrong E. 2015. Genomics Are Transforming Our Understanding of Responses to Climate Change, *BioScience* **65**: 237–246.

Storey JD, Tibshirani R. 2003, Statistical significance for genome wide studies. *PNAS.* **100**: 9440–9445.

Temunović M, Garnier-Géré P, Morić M, Franjić J, Ivanković M, Bogdan S, Hampe A. 2020. Candidate gene SNP variation in floodplain populations of pedunculate oak (*Quercus robur* L.) near the species' southern range margin: Weak differentiation yet distinct associations with water availability. *Molecular ecology* **29**: 2359-2378.

Theraroz A, Guadaño-Peyrot C, Archambeau J, Pinosio S, Bagnoli, F, Piotti, A, Avanzi C, Vendramin GG, Alía R, Grivet D, Westergren M, González-Martínez SC. 2024. The genetic consequences of population marginality: a case study in maritime pine. *Diversity and Distributions*, **e13910.**

Thompson J. **2020**. *Plant Evolution in the Mediterranean*. Oxford: Oxford University Press.

Thornton KR, Jensen JD. **2007**. Controlling the False-Positive Rate in Multilocus Genome Scans for Selection. *Genetics* **175**: 737–750.

Tintle NL, Borchers B, Brown M, Bekmetjev A. **2009**. Comparing gene set analysis methods on single-nucleotide polymorphism data from Genetic Analysis Workshop 16. *BMC Proceedings* **3**: 1–5.

Vangestel C, Eckert AJ, Wegrzyn JL, St. Clair JB, Neale DB. **2018**. Linking phenotype, genotype and environment to unravel genetic components underlying cold hardiness in coastal Douglas-fir (*Pseudotsuga menziesii* var. *menziesii*). *Tree Genetics and Genomes* **14**, 10.

Vilà-Cabrera A, Premoli AC, Jum AS. 2019. Refining predictions of population decline at species' rear edges. Global Change Biology **25**: 1549–1560.

Yan J, Wang B, Jiang Y, Cheng L, Wu T. **2014**. GmFNSII -Controlled Soybean Flavone Metabolism Responds to Abiotic Stresses and Regulates Plant Salt Tolerance. *Plant and Cell Physiology* **55**: 74–86.

Yang A, Dick CW, Yao X, Huang H. **2016**. Impacts of biogeographic history and marginal population genetics on species range limits: a case study of *Liriodendron chinense*. *Nature Publishing Group*: 1–12.

Yeap WC, Namasivayam P, Ooi TEK, Appleton DR, Kulaveerasingam H, Ho CL. **2019**. EgRBP42 from oil palm enhances adaptation to stress in Arabidopsis through regulation of nucleocytoplasmic transport of stress-responsive mRNAs. *Plant Cell and Environment* **42**: 1657–1673.

Yuan S, Shi Y, Zhou BF, Liang YY, Chen XY, An, QQ, Fan YR, Shen Z, Ingvarsson PK, Wang B. 2023. Genomic vulnerability to climate change in Quercus acutissima, a dominant tree species in East Asian deciduous forests. *Molecular ecology*, **32***:* 1639-1655.

9. LIST OF CAPTIONS

Figure 1. Location of the three main mountain ranges in the Sistema Central of the Iberian Peninsula (Spain) where the study was developed: Bejar (BJR), Gredos (GRD) and Guadarrama (GDM). The three-dimensional coloured map represents an example of the intra-range environmental classification in core (optimal) and marginal areas developed for *S. ciliata* based on ecological niche modelling and putative selective pressures (see Morente-López *et al*. 2022). In each of the three mountain ranges, two populations were selected, one in core (blue) and one in marginal (red) environmental conditions. The approximate locations of the two populations selected in Guadarrama mountain range, Pico de Peñalara (PEN) and Morrena Peñalara (MOR) are depicted in optimal and marginal areas respectively. Black shaded areas in the map represents elevations above 1,500 m. Dashed lines represent political divisions of provinces.

Figure 2. Demographic models tested in Fastsimcoal2. (a) Demographic models tested at population level. Model parameters are bottleneck (T_{BOT}) and expansion (T_{EXP}) times, current (N_{CUR}) and ancestral (N_{ANC}) effective population sizes and population size during the bottleneck event (N_{BOT}). (b) Demographic models tested at mountain range level. Additional model parameters are current population size of marginal (N_M) and core (N_O) populations, time of instantaneous isolation (T_{DIV}) and migration probability from marginal to core (M_{MC}) and core to marginal (M_{CM}) populations (horizontal arrows).

Figure 3. Population genetic structure of *S. ciliata* in the Sistema Central of the Iberian Peninsula (Spain) showing closer relationships between the two western mountain ranges (Gredos and Bejar) and separating the eastern Guadarrama mountain range. Refer to Table 1 for population acronyms. (A) Bayesian cluster analysis (fastStructure). Figure shows the individual bar plot grouped by population and mountain ranges. Bar colours represent individual assignment probability to each of the optimal K=2 groups. (B) Neighbour-net (Nnet) phylogenetic network constructed in SplitsTree v4. (C) Population relationships and migration edges inferred by TREEMIX. Arrows are coloured by migration weight and branch lengths are proportional to genetic drift. Notice that the only migration event linked two populations was found in Bejar and Gredos mountain ranges (NEG-CAM).

Figure 4. Parameters inferred from coalescent simulations with Fastsimcoal2 under the best-supported demographic model for single populations ("Bottleneck" model, see Figure 2a). For each parameter, the point estimate and the lower and upper 95% confidence intervals, generated by parametric bootstrapping, are shown. Model parameters include T_{BOT} (time when the bottleneck began), N_{CUR} and N_{ANC} (current and ancestral population sizes), and N_{BOT} (population size during the bottleneck event).

Figure 5. Parameters inferred from coalescent simulations with Fastsimcoal2 under the best-supported demographic model fitted at mountain range level ("Bottleneck and Isolation of two populations" model, see Figure 2b). For each parameter, the point estimate and the lower and upper 95% confidence intervals, generated by parametric bootstrapping, are shown. Model parameters include: T_{BOT} and T_{DIV} (bottleneck and instantaneous split times), N_M and N_C (current effective population size of marginal and core populations), N_{ANC} (ancestral population size), N_{BOT} (population size during the bottleneck event), and M_{MC} and M_{CM} (migration from marginal to core and core to marginal populations). The red and blue shades visualise the division of the ancestral population into marginal and core populations.

Figure 6. Diagram of the gene pathways tested for signals of selection. Five pathways (indicated with red names) were enriched with positive *alpha* values estimated by BayeScanHierarchical, indicating diversifying selection between populations inhabiting core and marginal environments. The size of the nodes (pathways) is proportional to the number of genes involved. The node colour scale represents the SUMSTAT score. A higher SUMSTAT score indicates stronger signals of polygenic selection within the pathway. Edges represent mutual overlap; nodes are connected if one of the sets has at least three of its genes in common with the other gene set. Edge width is proportional to the number of shared genes. Nodes marked with an asterisk indicate gene pathways that are plant-specific. For clarity, the figure represents only the 51 pathways with a SUMSTAT score higher than the median value of the entire dataset (N=86).

10. TABLES AND FIGURES

Table 1: *Silene ciliata* populations of the Sistema Central (Spain) used in the targeted resequencing experiment. Geographical and environmental characteristics and sample sizes (*N*) for the experiment are also provided.

Population (ID)	Mountain Range	Environment	*N*	Latitude	Longitude	Snowpack	MinT (°C)	Elevation (m)
Canchal Negro (NEG)	BJR	Core	15	40°20′20′′N	5°41′22′′W	0.59	-7.2	2360
Las Cimeras (RUI)	BJR	Marginal	16	40°21′07′′N	5°40′59′′W	0.27	-6.7	2000
Alto del Morezón (ZON)	GRD	Core	15	40°14′57′′N	5°16′08′′W	0.62	-7.7	2380
Los Campanarios (CAM)	GRD	Marginal	16	40°15′42′′N	5°12′55′′W	0.34	-6.0	2000
Pico de Peñalara (PEN)	GDM	Core	17	40°51′02′′N	3°57′24′′W	0.67	-7.8	2400
Morrena Peñalara (MOR)	GDM	Marginal	15	40°50′11′′N	3°57′01′′W	0.33	-5.7	1980

ID, identification of each population; Mountain Range, mountain range of origin: Bejar (BJR), Gredos (GRD) and Guadarrama (GDM); Environment, environmental classification; *N,* sample size; Latitude and Longitude, geographical coordinates; Snowpack, snowpack accumulation values in thaw months range from 0 to 1 (values close to 1 indicate deep snowpack, while values close to 0 indicate null snow cover; López-Moreno *et al.* 2007)); MinT, minimum annual temperature; Elevation, refers to the mean elevation (in meters above sea level) estimated for each population (variation in elevation within populations did not exceed 10 meters). Geographical and environmental information extracted from Morente-López et al. (2019). Based on Morente-López et al. (2022), the main putative selective pressures for *S. ciliata* are snowpack in the thaw months and minimum temperature. These variables were thus crucial to differentiate environmentally marginal and core areas.

30

Table 2. Nucleotide diversity, neutrality tests and inbreeding by population.

Pop/Env	L (bp)	Polymorphic sites		Nucleotide diversity		Neutrality tests			Inbreeding	
		N	%	Tajima's π	Watterson's θ	*TajD*	*FuD*	*FuF*	*F*	Relatedness
NEG/Cor	2,678,634	33,568	47.17	0.00346	0.00338	-0.073	-0.072	-0.077	-0.082	0.056
RUI/Mar	2,684,833	33,747	47.43	0.00337	0.00331	-0.092	-0.134	-0.130	-0.040	0.055
ZON/Cor	2,677,081	34,147	47.99	0.00338	0.00344	-0.231	-0.275	-0.282	-0.044	0.058
CAM/Mar	2,683,788	30,934	43.47	0.00329	0.00303	0.079	0.193	0.173	-0.069	0.053
PEN/Cor	2,679,723	38,336	53.87	0.00346	0.00370	-0.362	-0.471	-0.475	-0.059	0.051
MOR/Mar	2,676,981	34,631	48.67	0.00338	0.00349	-0.263	-0.263	-0.283	-0.041	0.058

TajD, Tajima's *D*; *FuD, Fu & Li's D*; FuF, Fu & Li's F*; F*, average inbreeding coefficient; Relatedness, average pairwise relatedness statistic (unadjusted A_{jk}), with values around zero indicating unrelated individuals.

Table 3. Candidate genes putatively under divergent selection detected in *Silene ciliata*. "Nº SNPs" refers to the number of SNPs detected with Arlequin (ARL) and BayeScanHierarchical approach (BAY). "Category" refers to the group of sequences to which the candidate gene belongs (See section "Selection of genes for sequencing"): A. Response to abiotic stimulus (GO: 0009628); F. Flower development (GO: 0009908); O. Candidate genes related to local adaptation to elevation in previous studies (Sacristán-Bajo *et al.* 2019). "Biological Processes" provides an overview of the main biological processes mediated by the candidate genes.

Gene Id (*S. ciliata*)	Nº SNPs ARL/BAY	Category	Description	Uniprot ID (Best Blast)	Gene ID (Best Blast)	Biological Processes
comp73228	1/1	FO	ATP sulfurylase 1	Q9LIK9	APS1	Hydrogen sulfide biosynthetic process; Response to cytokinin; Response to cadmium ion
m.101530	1/1	A	Oxygen-evolving enhancer protein 1. chloroplastic	P12359	PSBO	Photosystem II assembly and stabilization; response to light intensity, response to water deprivation
m.102611	1/1	FO	Transmembrane protein	Q0WQ99	At4g16850	petal development; positive regulation of cell population proliferation
m.137232	1/1	F	Nuclear-pore anchor	A4GSN8	NUA	Stamen development; Negative regulation of flower development
m.140709	1/1	O	BAG family molecular chaperone regulator 3	Q9LYP4	BAG3	Chaperone-mediated protein folding; positive regulation of cellular process, response to jasmonic acid, response to wounding
m.19977	6/2	FA	Cytochrome P450 71B37	Q9LIP3	CYP71B37	Oxidation-reduction process; response to jasmonic acid, response to wounding, tissue development
m.843	2/2	A	Indole-3-acetic acid-amido synthetase GH3.10	Q9ZNS2	GH3.10	Response to light stimulus
m.87654	1/1	O	Serine carboxypeptidase-like 49	P32826	SCPL49	Proteolysis involved in cellular protein catabolic process
m.8887	1/1	A	Usp domain-containing protein	A5C9Q0	VIT_08s0007g01430	Response to cold; Response to heat; Response to oxidative stress; Chaperone-mediated protein folding

Table 4. Candidate genes with evidence of selective sweeps for *Silene ciliata* in core or marginal populations. "Category" refers to the group of sequences to which the candidate gene belongs (See section "Selection of genes for sequencing"): A. Response to abiotic stimulus (GO: 0009628); F. Flower development (GO: 0009908); O. Candidate genes previously related to local adaptation to elevation in previous studies (Sacristán-Bajo *et al.* 2019).

Gene Id (*S. ciliata*)	Nº Selective sweeps	Category	Env.	Description	Uniprot ID (Best Blast)	Gene ID (Best Blast)	Biological Proccesess
m.133396	1	A	Marginal	Proteasome subunit beta type	Q8LD27	PBF1	Defence response to fungus, incompatible interaction; proteasomal protein catabolic; proteolysis
comp65047	3	A	Marginal Core	Poly(ADP-ribose) glycohydrolase	Q9SKB3	PARG1	Cellular response to DNA damage stimulus; Defence response to fungus; Regulation of DNA repair; Response to osmotic stress, oxidative stress and water deprivation; Rhythmic process; Stomatal closure
comp54123	1	O	Core	Carboxylate clamp type tetratricopeptide repeat protein	F4IRM4	PHOX1	Root hair cell development
comp64011	1	A	Core	DNA mismatch repair	F4JP48	MSH4	Homologous chromosome segregation; Mismatch repair
comp76868	1	F	Core	DNA repair protein	Q9SL02	RAD50	Gametophyte development; Chromosome organization involved in meiotic cell cycle; Telomere maintenance; DNA repair
m.117629	4	OF	Core	Protein TPLATE	F4J8D3	TPLATE	Endocytosis; Pollen development

m.141175	1	O	Core	Uncharacterized protein	A0A0K9RLQ1	SOVF_052510	na
m.28293	1	A	Core	Histone-lysine N-methyltransferase	Q8GZB6	SUVH4	Histone methylation; Maintenance of DNA methylation; Peptidyl-lysine methylation
m.45836	2	O	Core	FAD-binding FR-type domain-containing protein	A0A2P4H4H9	VITISV_024875	Oxidation-reduction process
m.48088	1	A	Core	Sucrose synthase Glycine max	P13708	SS	Nodulation; sucrose metabolic process
m.83703	1	A	Core	ULP_PROTEASE domain-containing protein	A0A0K9S186	SOVF_011010	Proteolysis

35

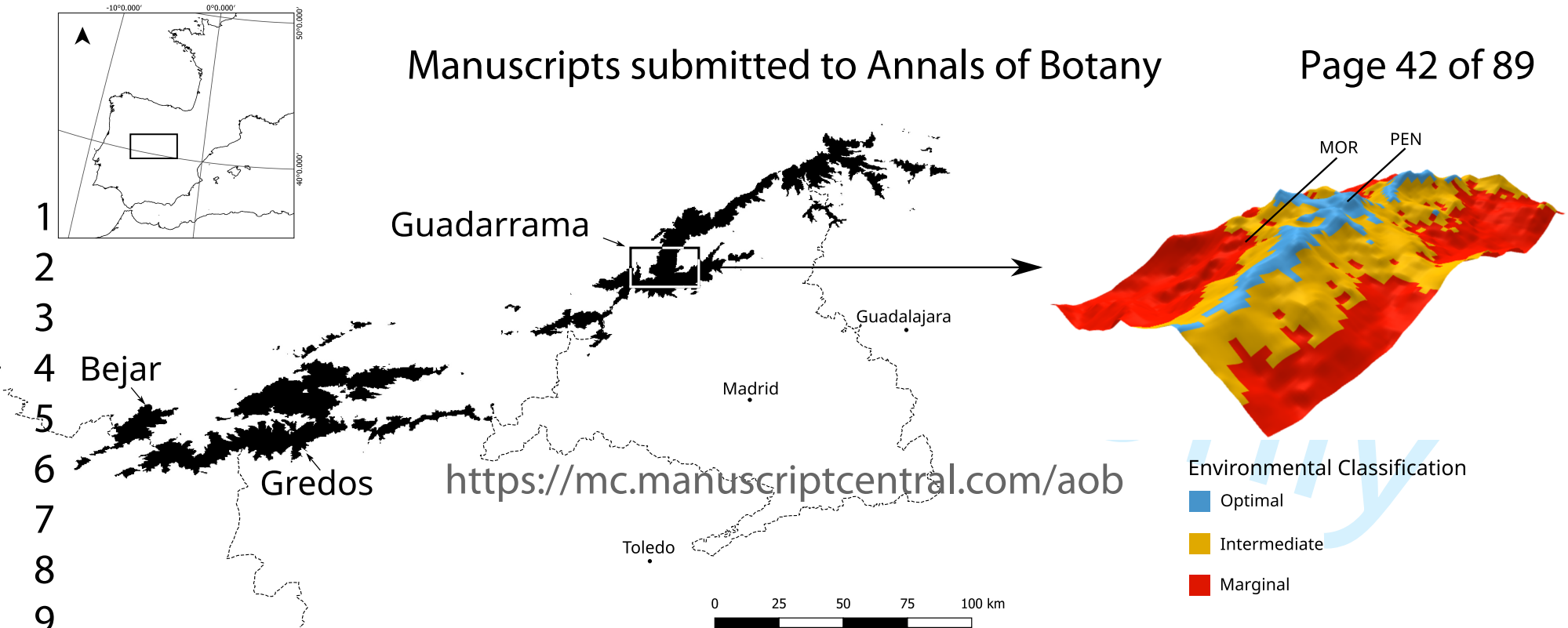

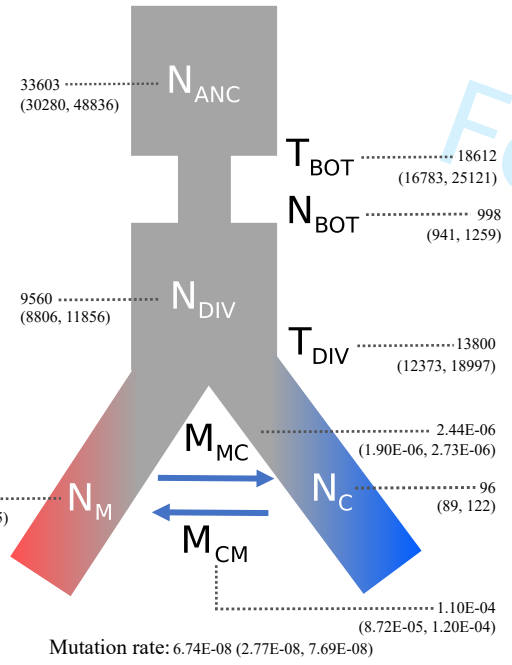

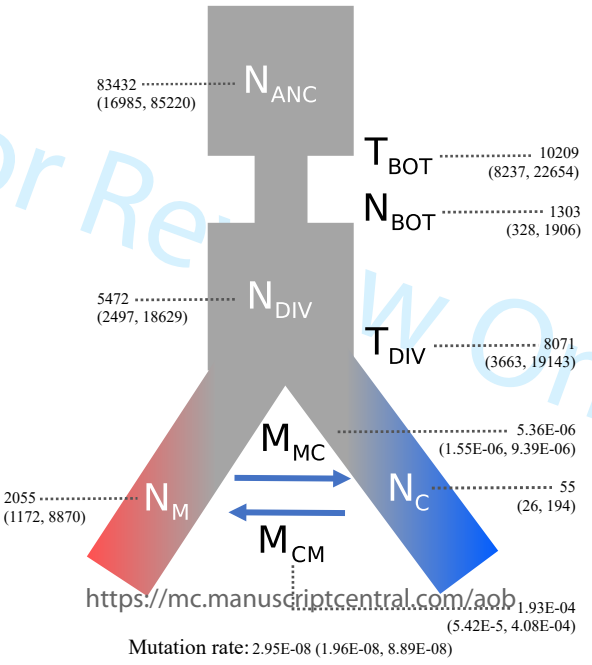

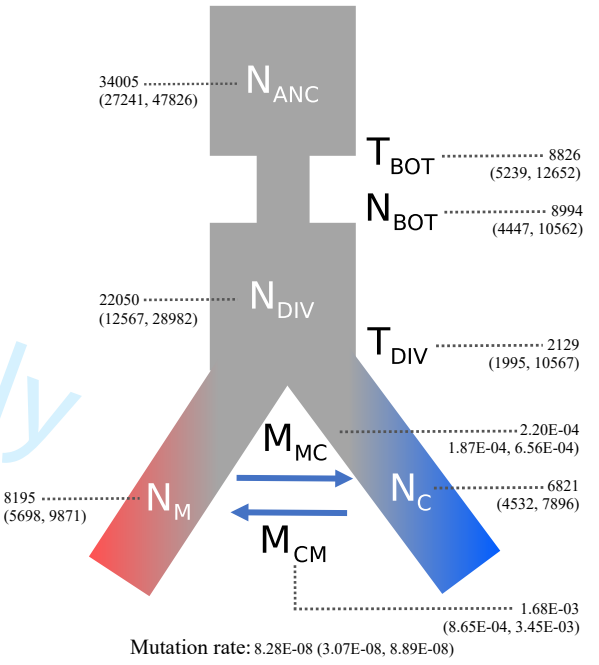

A)

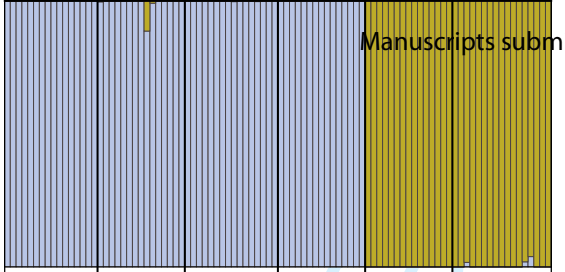

B)

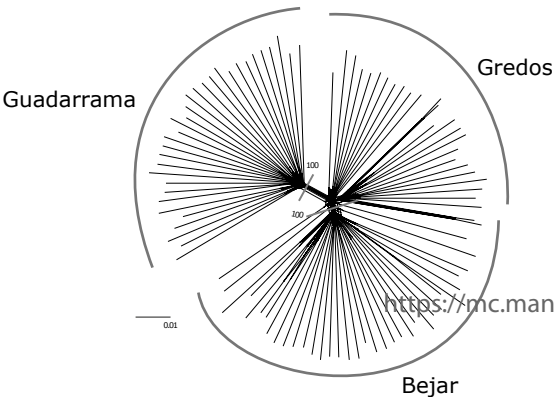

C)

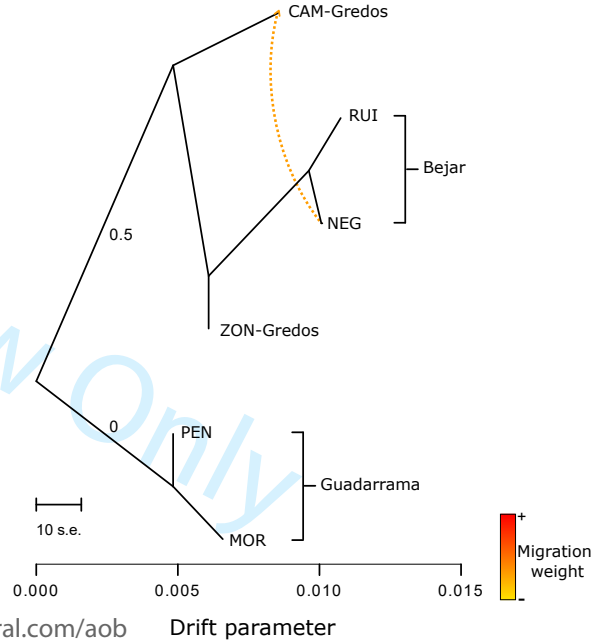

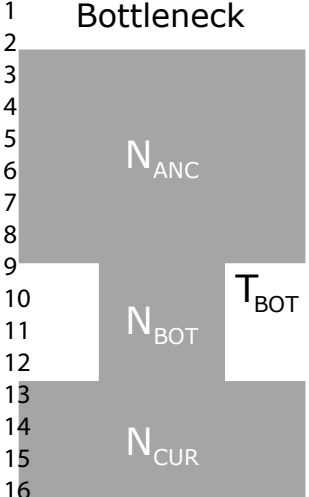

Pop/Env	N_{ANC}	N_{CUR}	Mutation Rate	N_{BOT}	T_{BOT}
NEG/Cor	27425 (15519, 95337)	316 (88, 512)	5.66E-08 (3.94E-09, 9.9E-08)	161 (38, 278)	7170 (4010, 9624)
RUI/Mar	29312 (16806, 77050)	393 (53, 613)	4.82E-08 (8.21E-09, 8.96E-08)	114 (20, 472)	7253 (3487-10830)
ZON/Cor	32872 (11390, 83357)	525 (92, 538)	5.24E-08 (2.32E-08, 7.92E-08)	403 (49, 336)	9479 (3684, 9597)
CAM/Mar	33805 (16610, 80001)	184 (119, 478)	6.55E-08 (1.75E-08, 8.5E-08)	138 (36-292)	4223 (3882, 10860)
PEN/Cor	69097 (18843, 94834)	158 (123, 647)	1.02E-07 (1.43E-08, 9.99E-08)	54 (38, 386)	5100 (3237, 9885)
MOR/Mar	62815 (28424, 84521)	400 (98, 577)	3.59E-08 (1.66E-08, 8.58E-08)	146 (29, 310)	9138 (3881, 9813)

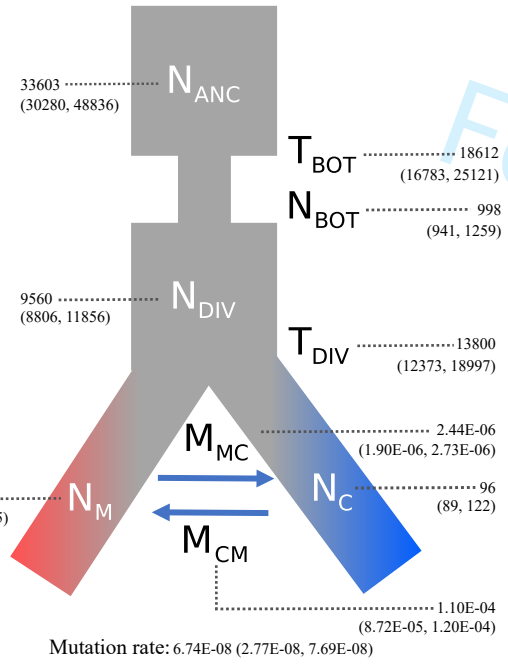

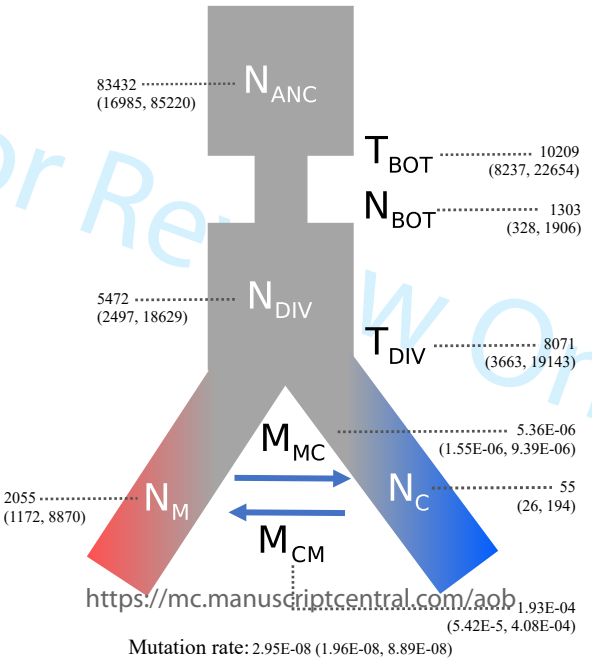

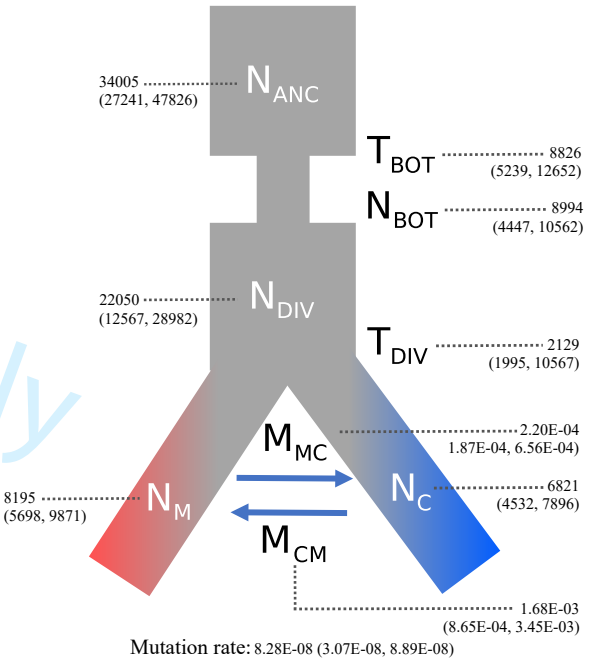

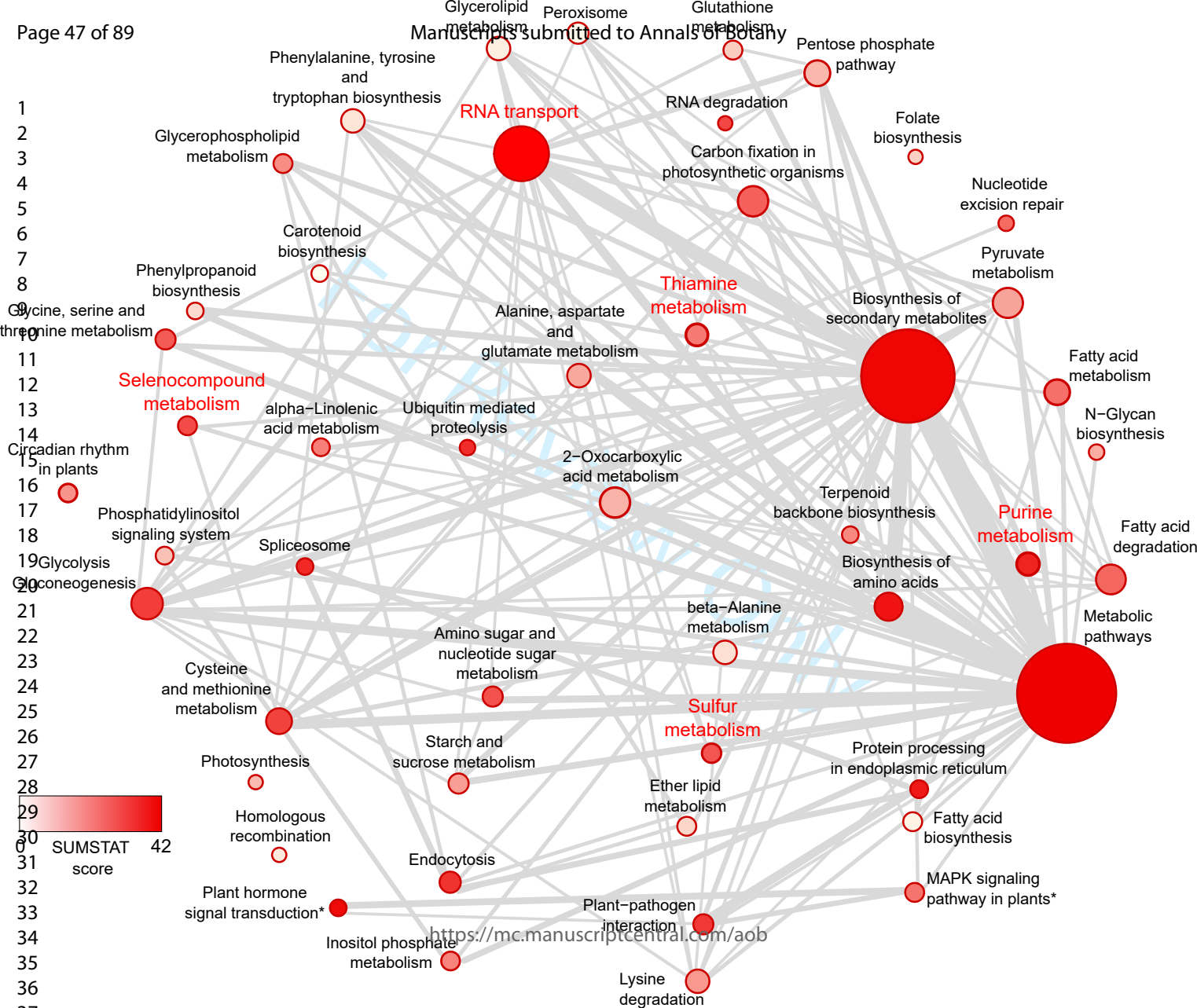

Original Article

ADAPTIVE VALUE OF MARGINAL POPULATIONS: INTEGRATING SELECTIVE SIGNALS, NEUTRAL PROCESSES AND TEMPORAL SCALES

Carlos Lara-Romero[1,2*], José M. Iriondo[1,2], Alfredo García-Fernández A[1,2], Javier Morente-López[3], Sandra Sacristán-Bajo[2], Santiago C. González-Martínez[4]

[1]Global Change Research Institute (IICG-URJC), Rey Juan Carlos University (URJC), Madrid, Spain.

[2] Department of Biology and Geology, Physics and Inorganic Chemistry. Rey Juan Carlos University (URJC), Madrid, Spain.

[3]Department of Plant Evolutionary Ecology, Goethe-University Frankfurt, Frankfurt am Main, Germany.

[4]INRAE, Univ. Bordeaux, BIOGECO, Cestas, France.

*Corresponding author: carlos.lara@urjc.es

Running title: ADAPTIVE VALUE OF MARGINAL POPULATIONS

1. ABSTRACT

Background and aims: The importance of populations inhabiting ecologically marginal areas has been extensively debated and shown to depend, to a large extent, on their adaptive value. In the context of climate change, their ecological originality can give marginal populations the capacity to generate unique gene combinations. In this study, we searched for evidence of genetic diversity of adaptive value in marginal populations, through a genomic analysis that encompasses a multidimensional approach, integrating selective signals, neutral processes and temporal scales.

Methods: We used a targeted exome sequencing approach to search for genomic signatures of divergent selection between environmentally marginal and core populations of the Mediterranean alpine species *Silene ciliata*. We also analysed their current genetic population structure and demographic history, as well as signatures of selective sweeps at different levels.

Key results: Populations from core and marginal environments presented similar values of nucleotide diversity, inbreeding, and relatedness. Demographic history played a more relevant role than current environmental conditions in explaining the levels of genetic diversity in marginal populations. We also detected putative signals of diversifying selection among populations inhabiting environmentally marginal and core areas, involving 11 SNPs located in nine genes, as well as five gene pathways.

Conclusions: Populations currently inhabiting marginal environments can diverge from ~~populations~~those occupying core areas due to local adaptation despite low overall genetic differentiation. The ~~availability~~presence of polymorphisms or traits adapted to specific environments in marginal populations ~~can~~may be particularly ~~helpful~~valuable in conservation management and restoration, especially in the context of changing ~~environments~~environmental conditions.

Key words: climate change, demographic inference, environmental gradients, divergent selection, gene pathways, genetic adaptation.

2. INTRODUCTION

Environmental heterogeneity induces key demographic, genetic and phenotypic differentiation within the natural ranges of species, leading to the identification of *core* and *marginal* areas (Soulé 1973; ~~Hardie and Hutchings 2010;~~ Pouget *et al.* 2013; Pironon *et al.* 2017). Core areas, characterized by prevalent and, presumably, optimal environmental conditions, host large and, often, genetically diverse populations. In contrast, marginal areas, with atypical and potentially restrictive environmental conditions, present a more complex scenario (Soulé 1973; Brown 1984).

Historically, marginal populations have been perceived as genetically impoverished and maladapted due to genetic drift and inbreeding, ~~and~~ thus harbouring little evolutionary potential (Lynch and Gabriel 1987; Lande 1994; Eckert *et al.* 2008a). However, evidence from some species suggests that these populations may be locally adapted to withstand specific environmental pressures. This makes them particularly valuable in the context of climate change, as their genetic diversity may confer adaptive advantages, enhancing the organisms' chances of survival and reproduction (Barrett and Schluter 2008; ~~Hoffmann and Sgró 2011;~~ Morente-López *et al.* 2021). Despite the contrasting views, most studies have been based on limited genetic information, lacking a genomic perspective (Stillman and Amstrong 2015; Razgour *et al.* 2019). Genomic approaches can help to identify unique adaptations in marginal populations as well as to forecast their responses to future environmental pressures (e.g., Theraroz *et al*. 2024).

Genetic adaptation is influenced not only by environmental pressures but also by available genetic diversity, past demographic history and gene flow (Kawecki 2008).

High levels of genetic diversity within populations are essential for natural selection and adaptation to take place. Demographic events like bottlenecks can reduce this diversity (Carbognani *et al*. 2019), while population growth can either diminish or augment it, depending on the influx of new genetic variants (Haghue and Routman 2016). Gene flow can either facilitate adaptation by boosting genetic diversity (Eckert *et al.* 2008b; ~~Hardie and Hutchings 2010;~~ Morente-López *et al.* 2021; Sacristán-Bajo et al 2025) or hinder it by introducing disadvantageous variants that are removed from the population by natural selection (Lenormand 2002).

When genetic adaptation is studied from a genomic perspective, the genomic signature of selection is superimposed on widespread signatures of the population's demographic history. For instance, both bottlenecks and population growth can generate nucleotide variation patterns that mimic selection (Barton and Etheridge 2004; Ramírez-Soriano *et al.* 2008). Hence, to identify adaptive genetic variants, it is imperative to employ modelling techniques capable of differentiating between the genetic signatures of selection and those stemming from neutral evolutionary processes (e.g., González-Martínez *et al.* 2017; Mayol *et al.* 2020; Evans *et al.* 2023).

Alpine ecosystems exhibit high environmental variability, leading to rapidly shifting selective pressures over short geographical scales (Byars *et al.* 2007; Morente-López *et al.* 2022). In this context, *Silene ciliata* Pourret, a well-studied Mediterranean alpine cushion plant, exemplifies key questions in ecology and evolution in marginal plant populations (García-Fernández *et al.* 2012; Lara-Romero *et al.* 2016; Morente-López *et al.* 2021, 2022). Field studies have shown lower longevity, lower proportion of flowering plants and fewer flowers, fruits, and seeds per plant in the lower-elevation populations (Giménez-Benavides *et al.* 2007; Giménez-Benavides *et al.* 2011). This results in declining growth rates in low-elevation populations ~~facing~~, which face local extinction,

while higher-elevation populations in more favourable environments ~~showed~~show stable growth rates (Giménez-Benavides~~, Albert, *et al.* 2011).~~ et al. 2011). In parallel, studies in common-garden conditions, have shown delayed flowering onset, peak and end (Morente-López et al., 2020), lower seed germination (Giménez-Benavides et al. 2007), and greater drought tolerance (García-Fernández et al., 2013) in low-elevation populations. Interestingly, ~~phenotypic and quantitative genetic~~additional research suggests that ~~these marginal~~ populations at lower elevations may possess adaptive advantages over their core counterparts~~, particularly in terms of germination, early establishment, and flowering phenology, which~~ that may be better suited to current and future climatic conditions (~~Giménez-Benavides, García-Camacho *et al.* 2011;~~ Morente-López *et al.* 2020, 2021). Furthermore, in the northern Mediterranean mountain ranges where the species occurs, the last ~~Pleistocene glaciations~~glacial maximum (LGM) have influenced the demographic dynamics and current distributions of many plant species (Feliner 2014; Carbognani *et al*. 2019; Evans *et al*. 2023; Pütz *et al.* 2024), although this aspect has not yet been studied in *S. ciliata*. This lack of knowledge is significant because demographic history could have influenced not only the current distribution of the species, but also the observed patterns of genetic adaptation. Understanding these patterns in mountain populations requires considering both the existence of LGM microrefugia and the dynamics of rear-edge and leading-edge populations (Hampe & Petit 2005; Opgenoorth *et al.* 2009; Vila-Cabrera *et al.* 2019). LGM microrefugia represent localized, climatically stable areas where species persisted during glacial periods, often corresponding to present-day rear-edge populations (Rull 2009). Rear edge populations, located at the oldest and most stable habitat margins, reflect ancestral conditions. In contrast, leading edge populations, found at the most recent and dynamic habitat margins,

reflect modern conditions and exhibit rapid adaptations to ongoing environmental changes (Hampe & Petit 2005; Vila-Cabrera *et al.* 2019).

In this study, we ~~sought~~aimed to ~~increase the evidence for~~assess the adaptive value of marginal populations through a genomic analysis that encompasses both selective and neutral processes, using a multiscale perspective that considers also recent and ancient processes. Our goal was to explore how past climatic fluctuations—particularly the LGM—and present-day environmental gradients have shaped the patterns of genomic variation in core and marginal populations. We sequenced 2,414 candidate genes in six natural populations (three core and three marginal), based on previous research that identified SNPs associated with environmental stress responses (Sacristán-Bajo *et al*. 2019). Using F_{ST}-outlier detection to assess long-term adaptation and selective sweep analyses for more recent events, we identified potentially adaptive variation ~~at~~across different timescales. Our ~~exploration~~analysis of adaptive genetic diversity extended to gene pathways to ~~explore~~investigate the role of gene networks in adaptation (Olson-Manning *et al*. 2012; Berg and Coop 2014; Exposito-Alonso *et al*. 2018). In addition, we examined spatial genetic structure and population dynamics using demographic inference models. To date, only a few studies have assessed the adaptive value of marginal populations using combined analyses of population genetic structure ~~analyses combined with,~~ demographic ~~inference models~~history and genomic signals of selection (e.g., Yang *et al*. 2016~~) or genomic analyses to identify signals of adaptation (e.g.,~~; Temunović *et al*. 2020; Yuan *et al*. 2023). Moreover, none has ~~used~~applied a multidimensional ~~approach that integrates~~framework integrating all ~~of~~ these perspectives. In our study, we asked the following questions:

1. Do core and marginal populations ~~have different~~differ in levels of genetic diversity, inbreeding or relatedness?

2. What is the spatial genetic structure of the studied populations? Which candidate genes and biological pathways ~~are potentially involved in explaining~~may underlie adaptive genetic differentiation between core and marginal populations?

3. Have there been abrupt changes in effective population sizes over time? If so, can they be ~~dated~~linked to the ~~last glacial period? And~~LGM, and are there genomic signatures (e.g., of selective sweeps) ~~that can be associated to adaptive processes driven by past environmental changes~~indicative of adaptation in either rear-edge or leading-edge contexts?

We hypothesised that distinct selective pressures operating on core versus marginal populations have driven genetic differentiation between ~~these groups~~them. We further ~~theorized~~expected that contemporary environmental stressors have accelerated ~~population~~demographic decline in marginal populations, ~~leading to reduced~~reducing their genetic diversity. ~~Additionally~~Finally, we expected that the ~~most recent glacial maximum~~LGM induced a severe demographic contraction, generating a genetic bottleneck ~~whose~~ signature ~~remains~~still detectable in ~~the~~present-day genetic variation ~~of the studied populations~~.

3. MATERIALS AND METHODS

3.1 Study species and populations

Silene ciliata Pourr. (Caryophyllaceae) is a dwarf cushion perennial plant that inhabits Mediterranean alpine habitats with marked environmental gradients. It has flowering stems that grow up to 15 cm tall, with each stem bearing 1 to 5 flowers. Its fruit capsules contain up to 100 seeds, which are dispersed by wind in August and September. The seeds are small, averaging 0.59 mg in mass and 1.1 to 1.5 mm in diameter, and lack specialized

dispersal structures, making the species primarily barochorous. Pollination is carried out by syrphid flies, bumblebees, and moths. The plant is self-compatible, but self-pollination is limited due to significant protandry (see Lara-Romero et al. 2014 and references therein). The distribution of *S. ciliata* comprises the mountain ranges of the Northern Mediterranean area from Spain to Bulgaria (Kyrkou *et al.* 2015), reaching its southernmost limit in the Sistema Central of the Iberian Peninsula (Spain). All *S. ciliata* populations from the Sistema Central are diploid and have the same phylogenetic origin, as shown by chloroplast DNA analysis (Kyrkou *et al.* 2015). In these areas, the species grows from 1,800 to 2,500 m in dry cryophilic pastures above the tree line. This Mediterranean Alpine ecosystem has a pronounced summer drought combined with high solar radiation, which typically selects for plant xerophytic traits.

At the end of the summer of 2013, we collected a minimum of thirty randomly selected plants from six populations located in three sub-mountain ranges of the Sistema Central (Spain): Guadarrama (GDM), Gredos (GRD) and Béjar (BJR) (Figure 1 and Table 1). All sampled plants were separated by at least two meters. The Sistema Central is a southwest-northeast oriented mountain range of approximately 500 km located in the centre of the Iberian Peninsula. ~~Guadarrama, Gredos~~GDM, GRD, and ~~Béjar~~BJR are in the western, central and eastern areas of the Sistema Central, respectively. The six studied populations were located at the high and low elevation margins of the sub-mountain ranges (Figure 1 and Table 1). Within each sub-mountain range, the populations were separated by distances ranging from two to four kilometers. High and low elevation margins represent core (optimal) and marginal environmental conditions, respectively, based on the study of the ecological niche and putative selective pressures for the species (Morente-López *et al.* 2022). According to Morente-López *et al*. (2022), core populations inhabit regions where habitat suitability equals or surpasses the highest 33rd percentile of the distribution

of ranked suitability values, estimated using the MaxEnt algorithm. Conversely, the marginal populations are found below the lowest 33rd percentile. In marginal populations, vegetation is dominated by dense shrub cover of *Cytisus oromediterraneus* Rivas Mart. et al. and *Juniperus communis* L. subsp. *alpina* (Suter) Celak. *S. ciliata* is restricted to small, isolated *Festuca curvifolia* Lag. ex Lange pastures, and populations are small, with at most a few hundred individuals. In contrast, core populations are extensive, dominated by *Festuca* fellfields with scarce shrubs, and support many thousands of individuals. Marginal populations are subject to shorter snow cover duration and higher minimum temperatures compared to core populations, reflecting the main climatic gradients relevant to the species (Morente-López *et al.* 2022). Cuttings were obtained from the collected plants, rooted and placed in pots in the Universidad Rey Juan Carlos CULTIVE experimental field (https://urjc-cultive.webnode.es). Resulting plants were grown in common garden conditions before DNA extraction in 2015. Further details on the common garden experiment are provided in Morente-López *et al*. (2020).

3.2 Selection of candidate genes for targeted sequencing

The annotated *Silene latifolia* Poir. and *S. ciliata* transcriptomes (GenBank references: GCA_900095335 and PRJNA528948, respectively; see Sacristán-Bajo *et al*. 2019) were used to design an exome capture experiment based on targeted sequencing. We sequenced a total of 2,414 candidate genes with high-confidence annotations. Candidate genes were selected considering three factors that address specific aspects related to genetic differentiation and adaptation in *S. ciliata*. The first set comprised 576 genes carrying SNPs with unusually high allele frequency differentiation between core and marginal populations (Sacristán-Bajo *et al.* 2019). Briefly, these SNPs were identified in a previous study based on 147,118 SNPs distributed along 12,688 sequences obtained from mRNA libraries of leaf tissue without any prior experimental treatment in common garden

conditions. The second set comprised 489 genes annotated with the Gene Ontology term "Flower development" (GO: 0009908) or any of the dependent and more specific terms. These genes are expected to be involved in the development of the flower over time, from its formation to its mature structure. This set of genes was selected because previous quantitative genetic studies in *S. ciliata* indicate the existence of important differences, probably related with contrasted selective pressures, in the flowering phenology of plants from marginal and core populations (Giménez-Benavides, García-Camacho, *et al.* 2011; Morente-López *et al.* 2020). Finally, the third set included 1,349 annotated genes associated with general processes that result in a change in state or activity of a cell or an organism because of an abiotic stimulus (GO: 0009628 or any of the more specific terms). This third set was included in the study to detect a broad range of new candidate genes under divergent selection not previously identified in *S. ciliata*, as previous work on the species was hampered by low statistical power and may have left much of the potential adaptive variants unidentified.

3.3 DNA extraction, targeted sequencing and SNP calling

We used the DNeasy Plant minikit (QIAGEN, Valencia, USA) to extract and isolate DNA from 94 plants (Table 1), 15-17 for each of the six studied populations. Library preparation covering the targeted sequences followed the manufacturer's protocol for Nugen SeqCap Developer kit. Samples were sequenced as 96-plex on a HiSeq2500 lane with paired-reads of 125 bp. Demultiplexing of reads was carried out with CASAVA 1.8.2 (Illumina Inc., San Diego, CA). Reads were masked for adapter contamination with *cutadapt* and low-quality bases were removed using *erne-filter* (ERNE v.1.4.5). Alignment was carried out with BWA MEM v.0.7.10 (https://github.com/lh3/bwa). The aligned sequences obtained from the targeted exome sequencing were deposited in GenBank with accession number PRJNA851086. Prior to SNP calling, alignments were

filtered for low mapping quality (<10) and reads were realigned around indels using GATK 3.6 (McKenna *et al.* 2010). SNP calling was performed on the entire sample simultaneously using the *UnifiedGenotyper* implemented in the GATK suite, which allowed the initial identification of ca. 185,000 SNPs.

Raw SNP data were filtered using VCFtools v0.1.14 (Danecek *et al.* 2011) and *vcffilter* function of VCFLIB (Garrison *et al.* 2022). Only biallelic SNPs with fewer than 20% missing data were kept. Indels were also removed from the dataset. SNPs were then filtered following the hard filtering suggested by GATK's user guide (https://gatk.broadinstitute.org/). This stringent filtering reduced the SNP dataset to 112,751 SNPs. Further, SNPs from paralogous genes were filtered combining two approaches. First, the SNP dataset was filtered by Hardy-Weinberg disequilibrium and polymorphism excess (Chen *et al.* 2014). To apply this filter, we estimated F_{IS} in sliding windows of 150 bp with a step of 50 bp. Sliding windows with an average F_{IS} lower than -0.5 were filtered (Hohenlohe *et al*. 2013; McKinney *et al.* 2017), which entailed the removal of 27,728 SNPs. Second, for the retained dataset (85,023 SNPs), we applied the *HDplot* method. *HDplot* combines information from the relative proportion of heterozygotes in a population (H) and the deviation of allele-specific reads of each locus from a 1:1 ratio (D), allowing the identification of paralogous loci throughout the range of allele frequencies (McKinney *et al.* 2017). A total of 13,362 SNPs (16%) with H greater than 0.65 and $|D| > 20$ were classified as located in paralogous sequence and subsequently removed, resulting in a final SNP dataset of 71,661 SNPs distributed in 2,278 genes.

3.4 Nucleotide diversity, population structure and demographic history

Nucleotide diversity, inbreeding and relatedness

Nucleotide diversity by population (Tajima's π and Watterson's θ) and standard neutrality tests (Tajima's *D*, and Fu & Li's *D** and *F**) were computed using mstatspop (https://github.com/CRAGENOMICA/mstatspop). Additionally, we estimated the number of polymorphic sites, average inbreeding coefficients (*F*) and pairwise relatedness (as evaluated by unadjusted A_{jk} statistic) for each population using VCFtools v0.1.14 (Danecek *et al.* 2011).

Population genetic structure

We investigated population genetic structure using the hierarchical analysis of molecular variance (AMOVA) implemented in Arlequin v3.5.2 (Excoffier and Lischer 2010). The analysis was conducted at three levels: (1) among mountain ranges; (2) between core and marginal populations within mountain ranges; and (3) within populations. Genetic differentiation was calculated for all three hierarchical levels, leading to estimates for F_{CT} (among mountain ranges), F_{SC} (between core and marginal populations within mountain ranges) and F_{ST} (among populations overall). F_{ST} was also calculated between all pairs of populations, and the significance levels of pairwise F_{ST} estimates were determined by permutation tests (10,000 permutations). Population genetic structure was also inferred by a Bayesian clustering method using fastStructure, with *K* groups from *K*=1 to *K*=6 (the number of localities in our sample), and the simple prior. For improved ancestry estimates and to identify subtle structure, the logistic prior was executed at values of *K* similar to those identified when using the simple prior. Then runs for *K*=2 and *K*=3 (the best *K*) were repeated ten times, and averaged *Q* values (i.e., the individual assignment probability to each of the *K* groups) were used to draw bar plots. As an alternative to AMOVA and fastStructure, we used a Neighbour-net phylogenetic network (NNet) constructed in SplitsTree v 4 (Huson and Bryant 2006), based on uncorrected_p distance with default parameters and 1,000 bootstraps. In order to account for gene flow while

inferring the relationships among *S. ciliata* populations, we also used TREEMIX v1.13 (Pickrell and Pritchard 2012). This method models patterns of both population splits and admixtures accessing the covariance structure of allele frequencies between populations and performing a Gaussian approximation for genetic drift, improving the fit of the inferred model by enabling migration edges. TREEMIX analyses were implemented with 500-SNP bootstrap resampling and considering a different number of migration events, ranging from zero to 10.

Demographic inference

Demographic inference at population level: An overall negative Tajima's *D* indicated an excess of low frequency polymorphisms (see Results), suggesting population growth. Based on these results, we tested multiple demographic models for each population separately using the coalescent approach implemented in Fastsimcoal2 v.2.6.0.2 (Excoffier *et al.* 2013). Fastsimcoal2 estimates the composite likelihood of a specific demographic scenario given the observed data as well as population genetic parameters such as divergence time, effective population size and gene flow, using the site frequency spectrum (SFS) as input. Un-folded site frequency spectra (calculated from observed counts of the derived allele) were generated separately for each of the six populations using VCF2SNPs (Liu *et al.* 2018). To maximize statistical power, we used all SNPs, including those in intragenic regions, for demographic inference, assuming most behave neutrally or quasi-neutrally. This assumption is supported by low levels of linkage disequilibrium (mean $r^2 = 0.11$) and a very small proportion of SNPs showing signatures of selection (see Results). We compared three demographic models (Figure 2). The first "Stationary" model represents a null model consisting in a population of constant size and is defined by a single parameter, the current population size (N_{CUR}). The second "Expansion" model is defined by three parameters: N_{CUR}, a time of instantaneous

population size change (T_{EXP}) and a population size prior to T_{EXP}. The third "Bottleneck" model is characterized by four parameters: N_{CUR}, a time ~~of instantaneous population size change~~at which the bottleneck began (T_{BOT}), a population size during the bottleneck event (N_{BOT}), and a population size prior to T_{BOT} (N_{ANC}). The duration of the bottleneck event was fixed at 100 generations to avoid problems associated with model overparameterization. We performed 100 independent runs for each population and demographic model consisting of 50 cycles of the Brent algorithm and 100,000 simulations. The maximum-likelihood runs under each model were then compared using AIC to select the optimal model for each population. Once the optimal model was identified, we estimated confidence intervals (CIs) by performing 100 parametric bootstraps based on best-model parameters. Mutation rate was estimated from the data assuming a generation time of two years, which reflects the time required for the plant to reach reproductive maturity (Giménez-Benavides~~, Albert,~~ *et al.* 2011).

Demographic inference at mountain range level: Previous studies have suggested historical environmental fluctuations related to glaciations affecting *S. ciliata* populations in central Spain (Morente-López *et al.* 2018). Glacial pulses would have been responsible for shifting *S. ciliata* populations to lower elevations. Postglacial recolonization of higher elevations from lower areas would have originated a front-advancing edge by a subset of the populations at lower elevation. To better understand the potential effect of environmental fluctuations during glaciations on *S. ciliata* populations, we used Fastsimcoal2 to statistically compare the relative fit of multi-population demographic models ("mountain models") incorporating three possible demographic scenarios involving both core and marginal populations (Figure 2b). The first model ("Isolation of two populations") was parametrised with the current population size of marginal (N_M) and core populations (N_O), and a time of instantaneous split (T_{DIV}) from a common

ancestral population (N_{ANC}); it represents a simple scenario without effective population size changes. The second model ("Bottleneck and Isolation of two populations") also considered the split of marginal and core populations from a common ancestral population but included a bottleneck event in the ancestral population prior to the split. This bottleneck event was modelled defining a time ~~of instantaneous population size change~~ when the bottleneck began(T_{BOT}), a population size during the bottleneck event (N_{BOT}) and a population size posterior to T_{BOT} (N_{DIV}). Finally, the third model ("Bottleneck and Divergence of a population") considered marginal populations as a result of a bottleneck in the ancestral population from which the core populations would have subsequently diverged; this model reflects the suggested glacial dynamics of the species in the Sistema Central mountain range described above. The three models included migration between marginal and core populations after the divergence event (M_{MC} and M_{CM}), as considering gene flow always improved model fitting (data not shown). The modelling set-up and assessment of model performance was the same as described for the models fitted at the population level.

3.5 Detecting distinct signatures of selection in marginal vs core populations

Hierarchical F_{ST}-outlier analyses

To investigate the contribution of natural selection to genetic adaptation in *S. ciliata,* we combined multiple approaches. First, we searched for signals of divergent selection at the single-locus (SNP) level using hierarchical F_{ST}-outlier analyses implemented in Arlequin and BayeScanHierarchical. For Arlequin, we ran 20,000 simulations under a hierarchical

island model with 100 demes per level to establish a null distribution. To control for false positives, we applied a False Discovery Rate (FDR) correction and considered loci with a $1–F_{ST}$ quantile < 0.05 as outliers (Storey et al 2003). BayeScanHierarchical, which extends the standard BayeScan Bayesian likelihood method to hierarchical population structure, was used to identify loci with strong evidence of selection (Foll *et al.* 2014). To ensure adequate statistical power, we set the minimum number of iterations to 10,000, the length of 20 pilot runs to 7,500 iterations, and the burn-in-length to 50,000 iterations. Loci having a *Q*-value (analogue to a FDR) lower than 5% were considered to be under strong selection.

Second, we estimated AFDs (Allele Frequency Differentials) between pairs of core and marginal populations. To reinforce the reliability of our results, we applied a strict criterion, considering a locus as a candidate for selection only if it was identified as an outlier by both hierarchical F_{ST} -outlier analyses and showed consistent AFD patterns across all three pairwise comparisons between core and marginal populations. For the AFD comparisons, the expected number of random significant tests was calculated by multiplying the number of SNPs tested by the probability of AFDs going in the same direction in each comparison by chance (0.5^3), indicating that several thousand SNPs could show consistent AFDs in the same direction by chance. However, combining AFDs with hierarchical F_{ST}-outlier detection at standard FDR of 0.05 allowed us to increase substantially the confidence in our results (FDR of combined test of 0.00625).

Detection of selective sweeps

To identify recent hard selective sweeps, we employed the SWEEPFINDER algorithm implemented in SweeD v.3.1 (Pavlidis *et al.* 2013). We chose to study hard selective sweeps for their capacity to reveal recent genetic adaptation responding to shifting environmental pressures. This method has the benefit to derive the null hypothesis from

the background pattern in the data itself, making it more robust to demographic events such as population growth (Nielsen *et al.* 2005; Pavlidis *et al.* 2013). For each gene, Composite Likelihood Ratios (CLRs) were calculated at 30 equally-spaced positions across the target genomic region. To increase statistical power, all CLR scans were run on unfolded SFS and monomorphic sites were included in the analysis (Pavlidis *et al.* 2013). To further increase power to detect selective sweeps, we only applied the test on 1,758 candidate genes that had 10 SNPs or more, which involved 52,740 SNPs. Significance thresholds for selective sweeps detected in each population were obtained by computing the distribution of CLRs in 100 data sets obtained by coalescence simulations in SFS_CODE (Hernandez 2008). The simulations were based in a demographic scenario of population expansion after a bottleneck, which was the most-likely demographic model in all the studied populations based on Fastsimcoal2 (see Results). To ensure a conservative approach, we only considered selective sweeps with higher likelihood than the maximum obtained in the simulations across all core and marginal populations.

Selection at the gene pathway level

We used a procedure developed in humans (Daub *et al.* 2013, 2017) and tested in plants (Mayol *et al.* 2020), to detect the joint effect of selection in biological pathways. For this purpose, we used KEGG Automatic Annotation Server to map our 2,278 candidate genes and retained 246 biological pathways that included at least four genes. This threshold was selected to provide sufficient statistical power for subsequent analyses while maintaining a reasonable number of pathways for biological interpretation. While a larger number of genes per pathway would provide greater statistical power, it would also significantly reduce the number of pathways analyzed. We refined this gene-pathway list by removing non-plant pathways (see a similar approach in Mayol *et al*. 2020), resulting in a final

selection of 86 known pathways in plants. Then, for the maximum value of the coefficient of selection *alpha* estimated by SweeD and BayeScanHierarchical, we performed a gene set enrichment approach as in Daub *et al*. (2013). For this purpose, we used the POLYSEL pipeline (https://github.com/CMPG/polysel). This pipeline calculates for each statistic the SUMSTAT score (Tintle *et al.* 2009), which is the sum of the values for that statistic of all genes in a given pathway. Then, the pipeline compares SUMSTAT scores, after different bias corrections, to a null normal distribution of 500,000 random sets created using a sequential random sampling method (Ahrens and Dieter 1985), with the same size as the original pathway. As in Daub *et al*. (2013), we reported the gene pathways that showed evidence of having collectively higher gene selection coefficients (Q-value < 0.2), which establishes a probability of finding up to 17 pathways falsely identified as significant by chance alone.

4. RESULTS

4.1 Nucleotide diversity, population structure and demographic history

Nucleotide diversity, inbreeding and relatedness

The comparison between core and marginal populations revealed minimal differences in genetic parameters. Nucleotide diversity, inbreeding and relatedness were similar for individuals in both environments (Table 2, all Wilcoxon rank tests: $P \geq 0.1$). Most

neutrality tests were negative (only CAM had a positive result; Table 2) indicating an excess of rare polymorphisms, which can be interpreted as a demographic signature of population expansion.

Population genetic structure

Three-level hierarchical analysis of molecular variance (AMOVA, Table S1) showed that most of the genetic variation (91.3%) was found within populations, though a significant portion of the variation (6.7%) occurred among mountain ranges. A small (2%) but significant genetic differentiation was detected between core and marginal populations within mountain ranges. Pairwise F_{ST} values were significant for all population pairs and ranged between 0.0155 and 0.1201 (Table S2), being higher for comparisons between mountain ranges (mean ± *SD*: 0.086 ± 0.030, *n*= 12) than within mountain ranges (0.022 ± 0.015, *n*=3). The optimal number of genetic groups in the Bayesian clustering analysis performed using fastStructure was *K*=2, with one group corresponding to Guadarrama and the other group corresponding to Bejar and Gredos (i.e., the westernmost) mountain ranges (Figure 3a). The Neighbour-net network (Nnet) exhibited three well defined groups corresponding with the three mountain ranges studied (Figure 3b). Within each mountain range group, individuals from marginal and core populations were not clearly differentiated. The disposition of the three groups within the network indicated that Gredos and Bejar are more closely connected between them than with Guadarrama. Such a partition is also supported by the TREEMIX graph (Figure ~~4e~~3c), which showed evidence of admixture between populations in Bejar (NEG) and Gredos (CAM), and a clear separation of those in Guadarrama (Figure 3c).

Demographic inference

Population level

For all populations, the model incorporating changes in population size due to bottlenecks and subsequent recent expansion ("Bottleneck" model in Figure 2a) was the most supported based on AIC differences (ΔAIC > 100 for all comparisons). In the highest-likelihood parameter set (Figure 4), estimates of ancestral population size (N_{ANC}) averaged 44,191 (range 27,425-69,097). The bottleneck started in all populations around 4,000–9,500 generations ago, which resulted in a strong reduction of the effective population size (mean N_{BOT} = 169, range 54-403). Current population size (N_{CUR}) had a mean of 329 (range 158-525) and represents an increase of between 30% and 75% over N_{BOT}. A recent population expansion was also supported for all populations except CAM by negative neutrality test values (Figure 4; see above).

Mountain range level

Regarding the models fitted for each mountain range, the "Bottleneck and Isolation of two populations" model (Figure 2b) had the lowest AIC scores (ΔAIC > 1500 for all comparisons). The highest-likelihood parameter set (Figure 5) suggests that ancestral populations suffered a bottleneck around 9,000-18,500 generations ago, which reduced drastically their effective population size. After the bottleneck, ancestral populations recovered up to 65% of their previous effective population size. Populations inhabiting current core and marginal areas within each mountain range subsequently diverged around 2,129–13,800 generations ago. After divergence, core and marginal populations were connected by low (i.e., near zero) and asymmetrical gene flow, with higher gene flow from core to marginal populations (mean M_{CM} = 6.62 E-04 *vs*. mean M_{MC} = 7.59 E-05). Estimates of current population sizes were systematically higher for marginal (mean N_{CUR} = 4,900, range 2,055-8,195) than for core populations (mean N_{CUR} = 2,324, range 55-6,821). Estimates of N_{CUR} were also notably lower for westernmost mountain ranges

(55 and 96 for Bejar and Gredos, respectively) than for eastern Guadarrama mountain range (6,821).

4.2 Detecting signatures of selection in marginal *vs* core populations

SNP and gene region level

The hierarchical island model in Arlequin identified 750 SNPs as significant F_{ST} outliers ($P < 0.05$ after FDR correction). Out of them, 35 SNPs showed consistent AFDs in all comparisons between pairs of core and marginal populations. Candidate SNPs belonged to 13 different genes. BayeScanHierarchical detected 170 outlier SNPs and 13 of these (belonging to 11 genes) showed consistent AFDs. Eleven SNPs located on nine genes were outliers using both methods (Table 3), and we considered them as potential candidate loci under divergent selection. These potentially adaptive SNPs/genes are involved in regulation of flower development, oxidation-reduction processes, response to light stimulus, UV protection and different stress responses (Table 3). Out of the nine genes, four were among those associated with adaptation to elevation in previous studies (Sacristán-Bajo *et al.* 2019), four were annotated as GO: 0009628 (response to abiotic stimulus) and two as GO: 0009908 (flower development) (Table 3).

Overall, composite likelihood ratio tests (CLRTs) found slightly more selective sweeps in core populations (mean = 1,303, range 698-2,478) than in marginal ones (mean = 1,186, range 559-2,346). Eighteen selective sweeps located in 10 genes were found in all the populations of the same type (Table 4) and were thus considered as potential candidate gene regions under selection in either marginal or core environments. From them, nine of the 10 genes were found in core populations and only one gene was systematically found in all marginal populations. Only three selective sweeps located in the same gene (PARG1, coding for a poly(ADP-ribose) glycohydrolase) were found in all the studied populations (Table 4). None of the genes with signs of a selective sweep experienced

divergent selection according to F_{ST}-outlier analyses (Tables 3 and 4). Five and four of them were involved in different biological processes associated with responses to abiotic stimulus (GO: 0009628) and flower development (GO: 0009908), respectively, and three were among the candidate genes associated with adaptation to elevation in previous studies (Sacristán-Bajo *et al.* 2019; Table 4).

Gene pathway level

A total of 1,623 out of 2,250 genes mapped on existing KEGG pathway maps for plants (Table S3). Mapped genes were distributed on 86 distinct pathways (Table S3). Five pathways, involving 47 candidate genes, were enriched for positive values of *alpha* estimated by BayeScanHierarchical (Q-value < 0.2; Table 4, Table S3) indicating diversifying selection between core and marginal populations. A low proportion of candidate gene pathways shared genes, with 42 out of the 47 genes being specific to only one of the five pathways. None of these genes were among those found significant in analyses at single-gene level (considering both F_{ST} outliers and selective sweeps; Tables 3 and 4, respectively). Enrichment analysis using the maximum value of *alpha* estimated by SweeD did not detect any biological pathways with significant SUMSTAT scores.

5. DISCUSSION

Remarkably, we found low genetic differentiation between core and marginal populations of *S. ciliata*, suggesting that both environments harbour a wealth of genetic variation on which selection could act. The similar levels of genetic diversity observed ~~between core and marginal populations could, in part, be explained by historical evolutionary processes, such as past~~may reflect the complex demographic history of the species,

including range shifts, expansions, and contractions ~~linked to~~ associated with climatic ~~changes, which have~~oscillations during and following the LGM. These historical processes likely shaped the current distribution of genetic ~~landscape of these~~diversity in *S. ciliata*, enabling both core and marginal populations~~.~~ to retain adaptive potential. This ~~finding~~ challenges the conventional view that marginal populations are genetically impoverished~~. Instead, our results suggest that these populations retain valuable adaptive genetic variation that could be essential for responding to~~ and stresses their role in future responses to environmental challenges~~.~~ (Morente-López *et al.* 2021, 2022).

Based on current declining growth rates, we hypothesized that *S. ciliata* populations inhabiting marginal areas might be genetically impoverished and lack adaptive value (Lynch and Gabriel 1987; Lande 1994; Eckert *et al.* 2008a). Instead, our study revealed an unexpected homogeneity in nucleotide diversity, inbreeding, and relatedness across populations, irrespective of their environmental conditions. Moreover, populations in marginal environments exhibit larger current population size (N_{CUR}), as estimated by historical demography models. This similarity in genetic parameters challenges preconceptions: rather than being genetically deprived, marginal populations possess genetic diversity comparable to their core counterparts. Genetically-based phenotypic differentiation between core and marginal populations, as previously documented (García-Fernández *et al*. 2012; Morente-López *et al*. 2020, 2022; Prieto-Benítez *et al*. 2021), together with the presence of genomic adaptive divergence in marginal populations (see Results), emphasize the adaptive value of *S. ciliata* marginal populations. While these marginal populations retain adaptive genetic diversity, climate change heavily impacts their survival. Environmental conditions at low elevations are constraining the viability of the populations, as evidenced by present-time demographic studies showing declining growth rates and higher local extinction risks at low elevations

compared to the stable growth rates in higher elevations ~~-~~(Giménez-Benavides~~, Albert~~ *et al*. 2011; Lara-Romero *et al*. 2014, 2016). Although available adaptive genetic diversity seems not to be enough to adapt to their changing environment, it still may facilitate the adaptation of higher-elevation populations through adaptive gene flow, as shown in empirical studies (Morente-López *et al*. 2021; Prieto-Benítez *et al*. 2021).

Demographic inferences support a bottleneck around the last ~~glaciation~~glacial maximum and subsequent divergence of populations in core and marginal environments. This divergence is plausible even at small spatial scales, given the species' limited dispersal capacity (Lara-Romero et al. 2014) and the potential for genetic isolation in heterogeneous landscapes, even despite spatial proximity (Budde et al. 2024). While some populations descended to lower elevations, others likely persisted on mountaintops~~, possibly~~ in ~~protected microhabitats~~climatically stable microrefugia (Feliner 2014; Thompson 2020; Pütz *et al*. 2024). These mountaintop populations, consistent with the concept of rear-edge populations (Hampe and Petit 2005; Opgenoorth et al 2009), show~~2024). This persistence in microrefugia would explain the~~ lower historical population size (N_{ANC}~~) in current mountaintop core populations (Carbognani *et al* 2019) and their~~), marked genetic divergence from ~~low-elevation~~marginal populations~~,~~ (as reflected by significant F_{SC} ~~between core and marginal populations. The~~), and a higher number of selective sweeps ~~in core populations further supports this scenario, indicating more ancient populations that have undergone~~. These genomic signatures suggest long-term persistence and multiple episodes of positive selection in isolated and stable microrefugia (Colonna *et al*. 2014; ~~Harris~~Carbognani *et al*. ~~2020~~ 2019; Deng *et al*. 2021).

~~Our~~In contrast, our results ~~also~~ suggest that marginal low-elevation populations experienced past expansions~~, driven by~~ during more favourable ~~environmental conditions.~~climatic periods, consistent with the leading-edge dynamics of colonisation

into newly suitable environments (Hampe & Petit, 2005). However, progressive warming over the last century has displaced the species' climatic optimum ~~towards higher elevations (Sanz-Elorza *et al.* 2003; Giménez-Benavides *et al.* 2007), explaining current demographic patterns~~upslope (Giménez-Benavides *et al.* 2007; Morente-López et al 2022), leading to current demographic declines in these now trailing-edge populations (Giménez-Benavides *et al.* 2007; Lara-Romero *et al*. 2014; Morente-López *et al*. 2022). ~~This scenario represents a 'rear-edge' situation (sensu Hampe and Petit 2005), where populations at the low-elevation edges played a crucial role in maintaining species'~~Despite this, their adaptive genetic diversity ~~and facilitating adaptation to environmental changes. This result questions the~~may still contribute to the evolutionary potential of core populations through adaptive gene flow (Morente-López et al 2021; Prieto-Benítez et al 2022). These findings question typical assumptions about a direct relationship between genetic ~~variation~~diversity, range limits and current environmental suitability, ~~suggesting that~~highlighting instead the influence of past demographic history ~~may still be more important than current environmental conditions~~ in shaping present-day genetic ~~diversity~~ patterns (Duncan *et al.* 2015; Pironon *et al.* 2015; Yang *et al.* 2016).

The macroevolutionary forces shaping the distribution and diversity of *S. ciliata* have also influenced microevolutionary processes, such as selection on specific genes and pathways. With respect to individual genes, we detected signals of selection in four genes related with flower development (*APS1, NUA, CYP71B37, atg4*). Previous work at the phenotypic level suggested local adaptation for phenological traits in association with elevation (Giménez-Benavides, García-Camacho, *et al.* 2011; Morente-López *et al.* 2020). This is an expected result since in alpine ecosystems flowering phenology is a crucial demographic event (Molau *et al.* 2005; Sedlacek *et al.* 2015), forcing plants to have a fine phenological adjustment to the climate (Scheepens and Sto 2013). Moreover,

we also identified candidate genes relevant for abiotic stress response in our study (Table 2). These include *PSBO* and *SCPL49*, recognized as drought-stress response genes (Ashburner and The Gene Ontology Consortium 2000; Berardini *et al.* 2015; Shaar-moshe *et al.* 2015), or *GH3*, which controls hypocotyl elongation, a molecular mechanism critical for germination and seedling establishment (Berardini *et al.* 2015).

Beyond the level of individual genes, our analysis revealed that adaptation in *S. ciliata* involves complex genetic mechanisms, including selection acting on five metabolic pathways. Four of them were involved in essential metabolic functions that are critical for plant survival, namely thiamine, purine, sulfur and seleno compound metabolisms. Abiotic stress alters plant metabolism, inducing biochemical and physiological responses that create tolerance (reviewed in Ramakrishna and Gill 2019). These metabolic adjustments involve fine regulations of several metabolic pathways including those identified here (Lawlor and Cornic 2002; Yan *et al.* 2014; Heinemann and Hildebrandt 2021). The other gene pathway was related to RNA transport from the nucleus to the cytoplasm, which plays pivotal roles in regulation of gene expression. Several studies support the important role that mRNA export mechanisms play in abiotic stress responses of plants (Chinnusamy *et al.* 2008; Ehrnsberger *et al.* 2019; Yeap *et al.* 2019). The detection of this signal at the pathway level suggests that adaptation in species with complex evolutionary histories may involve genetic traits controlled by multiple genes within specific pathways. This challenges the traditional view of adaptation as being driven by single-gene mutations. Remarkably, approaches focused on single loci failed to detect signatures of selection for any of the genes involved in these pathways. Because of their small effect-sizes, genes under "soft" selection are hard to detect by single-locus approaches, although together they can have a large impact on a biological pathway (Olson-Manning *et al.* 2012; Berg and Coop 2014).

The candidate genes and pathways identified in this study offer an initial understanding of the molecular mechanisms underlying the adaptive responses to marginal and core environments. However, it is crucial to consider the possibility of false positives. Notably, certain candidate genes revealed multiple significant SNPs, with some of these genes also previously suggested as potentially involved in adaptation in an RNAseq experiment (Sacristan *et al.* 2019). In addition, our strategy was guided by a focus on adaptive molecular signals concurrently identified in the three replicated elevation gradients, aiming at minimizing the occurrence of false positives (Thornton and Jensen 2007). Nevertheless, further confirmation is necessary to ascertain the adaptive nature of candidate genes and pathways, requiring additional research to establish a clear link between allelic variation and fitness (e.g., Jaramillo-Correa *et al.* 2015; Vangestel *et al.* 2018~~; Nagasaka *et al.* 2022).~~

Conclusions

Our findings ~~reject~~rejected the hypothesis that marginal populations of *S. ciliata* are genetically impoverished. ~~Conversely~~Instead, they revealed similar levels of genetic diversity in both core and marginal populations, shaped by historical events, with standing genetic variation in marginal populations being essential for adaptation to ~~on-going~~ongoing climate change. By employing a genomic analysis ~~encompassing~~that encompassed both selective and neutral processes, and adopting a multiscale perspective that ~~considers~~considered both recent and ancient ~~processes~~dynamics, we provided evidence of past selection in both environments and identified genes potentially associated with flower development and abiotic stress responses. Notably, genetic variation in *S. ciliata* may have partly ~~result~~resulted from selection acting on key metabolic pathways, which ~~underscores~~highlighted complex mechanisms of adaptation. ~~Additional~~Further research is needed to validate ~~these genes'~~the adaptive

role and fitness effects of these genes, as well as to assess the potential of *S. ciliata* populations to respond to future environmental pressures.

6. FUNDING

This work was supported by projects AdAptA (CGL2012-33528) of the Spanish Ministry of Economy and Competitiveness (MINECO). CLR was supported by a "Juan de la Cierva Incorporación" post-doctoral fellowship (Spanish Ministry of Science: IJC2019-041342-I), by the José Castillejo Mobility Programme for Young Doctors (Spanish Ministry of Science, Innovation and Universities, CAS18/00189) and by a Mobility Grant of COTE Cluster of Excellence granted by Université de Bordeaux. SSB was supported by a FPI pre-doctoral fellowship (MINECO: BES-2017-082317).

7. ACKNOWLEDGEMENTS

Niklaus Zemp from the ETH Zurich Genetic Diversity Centre for providing access to the reference transcriptome of *Silene latifolia*. Alex Widmer from ETH Zurich for his contribution to the design of the experiment. Samples were sequenced by IGA Technology Services (http://www.igatechnology.com). CLR, JML, AGF and JMI designed the experimental study, conducted the fieldwork, and collected the samples. JML with the help of CLR, AGF and JMI performed common garden experiments. CLR, SSB and AGF performed the DNA extractions in the laboratory. CLR and SGM analysed data with the help of SSB and AGF. CLR, SGM and JMI wrote the paper. All authors reviewed the paper and approved the final manuscript.

8. LITERATURE CITED

Ahrens JH, Dieter U. **1985**. Sequential random sampling. *ACM Transactions on Mathematical Software (TOMS)* **11**: 157–169.

Ashburner M, The Gene Ontology Consortium. **2000**. Gene Ontology : tool for the. *Nature Genetics* **25**: 25–29.

Barrett RDH, Schluter D. **2008**. Adaptation from standing genetic variation. *Trends in Ecology and Evolution* **23**: 38–44.

Barton NH, Etheridge AM. **2004**. The Effect of Selection on Genealogies. *Genetics* **166**: 1115–1131.

Berardini TZ, Reiser L, Li D, *et al.* 2015. The Arabidopsis Information Resource : Making and Mining the " Gold Standard " Annotated Reference Plant Genome. *Genesis* **53**: 474–485.

Berg JJ, Coop G. **2014**. A Population Genetic Signal of Polygenic Adaptation. *PLoS Genetics* **10**: e1004412.

Brown J. **1984**. On the relationship between abundance and distribution of species. *The American Naturalist* **124**: 255–279.

Byars SG, Papst W, Hoffmann AA. **2007**. Local adaptation and cogradient selection in the alpine plant, *Poa hiemata*, along a narrow altitudinal gradient. *Evolution* **61**: 2925–2941.

Budde KB, Rellstab C, Heuertz M, Gugerli F, Hanika T, Verdú M, Pausas JG, González-Martínez, S. C. 2024. Divergent selection in a Mediterranean pine on local spatial scales. *Journal of Ecology*, **112**, 278-290.

Carbognani M, Piotti A, Leonardi S, Pasini L, Spanu I, Vendramin GG, Tomaselli M, Petragliad A. 2019. Reproductive and genetic consequences of extreme isolation in *Salix herbacea* L. at the rear edge of its distribution. *Annals of Botany* **124**: 849-860.

Chen N, Van Hout ~~C V.,~~CV, Gottipati S, Clark AG. **2014**. Using mendelian inheritance to improve high-throughput SNP discovery. *Genetics* **198**: 847–857.

Chinnusamy V, Gong Z, Zhu J. **2008**. Nuclear RNA export and its importance in abiotic stress responses of plants. *Current Topics in Microbiology and Immunology*: 235–255.

Colonna V, Ayub Q, Chen Y, *et al.* 2014. Human genomic regions with exceptionally high levels of population differentiation identified from 911 whole-genome sequences. *Genome Biology* **15**: 1–14.

Danecek P, Auton A, Abecasis G, *et al.* 2011. The variant call format and VCFtools. *Bioinformatics* **27**: 2156–2158.

Daub JT, Hofer T, Cutivet E, *et al.* 2013. Evidence for polygenic adaptation to pathogens in the human genome. *Molecular Biology and Evolution* **30**: 1544–1558.

Daub JT, Moretti S, Davydov II, Excoffier L, Robinson-Rechavi M. **2017**. Detection of pathways affected by positive selection in primate lineages ancestral to humans. *Molecular Biology and Evolution* **34**: 1391–1402.

Deng J, Assandri G, Chauhan P, *et al.* 2021. Wolbachia - driven selective sweep in a range expanding insect species. *BMC Ecology and Evolution* **21**: 181.

Duncan SI, Crespi EJ, Mattheus N, Rissler L. 2015. History matters more when explaining genetic diversity within the context of the core–periphery hypothesis SARAH. *Molecular Ecology* **24**: 4323–4336.

Eckert CG, Samis KE, Lougheed SC. 2008a. Genetic variation across species' geographical ranges: The central-marginal hypothesis and beyond. *Molecular Ecology* **17**: 1170–1188.

Eckert CG, Samis KE, Lougheed SC. 2008b. Genetic variation across species' geographical ranges: The central-marginal hypothesis and beyond. *Molecular Ecology* **17**: 1170–1188.

Ehrnsberger HF, Grasser M, Grasser KD. 2019. Nucleocytosolic mRNA transport in plants: Export factors and their influence on growth and development. *Journal of Experimental Botany* **70**: 3757–3763.

Evans A, de Kort H, Brys R, Duffy KJ, Jersáková J, Kull T, Selosse MA, Tsiftsis S, Minasiewicz J, Jacquemyn H. 2023. Historical biogeography and local adaptation explain population genetic structure in a widespread terrestrial orchid. *Annals of Botany* 131: 623–634.

Excoffier L, Dupanloup I, Huerta-Sánchez E, Sousa VC, Foll M. 2013. Robust Demographic Inference from Genomic and SNP Data. *PLoS Genetics* **9**.

Excoffier L, Lischer HEL. 2010. Arlequin suite ver 3.5: A new series of programs to perform population genetics analyses under Linux and Windows. *Molecular Ecology Resources* **10**: 564–567.

Exposito-Alonso M, Vasseur F, Ding W, Wang G, Burbano HA, Weigel D. 2018. Genomic basis and evolutionary potential for extreme drought adaptation in Arabidopsis thaliana. *Nature Ecology and Evolution* **2**: 352–358.

Feliner GN. 2014. Patterns and processes in plant phylogeography in the Mediterranean Basin. A review. *Perspectives in Plant Ecology , Evolution and Systematics* **16**: 265–278.

Foll M, Gaggiotti OE, Daub JT, Vatsiou A, Excoffier L. 2014. Widespread signals of convergent adaptation to high altitude in Asia and America. *American Journal of Human Genetics* **95**: 394–407.

García-Fernández A, Iriondo JM, Escudero A. 2012. Inbreeding at the edge: Does inbreeding depression increase under more stressful conditions? *Oikos* **121**: 1435–1445.

García-Fernandez A, Iriondo JM, Bartels D, Escudero A. 2013. Response to artificial drying until drought-induced death in different elevation populations of a high-mountain plant. Plant Biology 15:93-100.

Garrison E, Kronenberg ZN, Dawson ET, Pedersen BS, Prins P. 2022. A spectrum of free software tools for processing the VCF variant call format: vcflib, bio-vcf, cyvcf2, hts-nim and slivar. *Plos Computational Biology 18*: e1009123.

Giménez-Benavides L, Albert MJ, Iriondo JM, Escudero A. **2011**. Demographic processes of upward range contraction in a long-lived Mediterranean high mountain plant. *Ecography* **34**: 85–93.

Giménez-Benavides L, Escudero A, Iriondo JM. **2007**. Reproductive limits of a late-flowering high-mountain Mediterranean plant along an elevational climate gradient. *New Phytologist* **173**: 367–382.

~~**Giménez-Benavides L, García-Camacho R, Iriondo JM, Escudero A. 2011**. Selection on flowering time in Mediterranean high-mountain plants under global warming. *Evolutionary Ecology* **25**: 777–794.~~

González-Martínez SC, Ridout K, Pannell JR. **2017**. Range Expansion Compromises Adaptive Evolution in an Outcrossing Plant. *Current Biology* **27**: 2544-2551.e4.

Haghue M, Routman E. **2016**. Does population size affect genetic diversity? A gest with simpatric lizard species. *Heredity* **116**: 92-98.

Hampe A, Petit RJ. 2005. Conserving biodiversity under climate change: the rear edge matters. *Ecology letters*, **8:** 461-467.

~~**Hardie DC, Hutchings JA. 2010**. Evolutionary ecology at the extremes of species' ranges. *Environmental Reviews* **18**: 1–20.~~

~~**Harris RB, Irwin K, Jones MR, *et al.* 2020**. The population genetics of crypsis in vertebrates: recent insights from mice, hares , and lizards. *Heredity* **124**: 1–14.~~

Heinemann B, Hildebrandt TM. **2021**. The role of amino acid metabolism in signaling and metabolic adaptation to stress-induced energy deficiency in plants. *Journal of Experimental Botany* **72**: 4634–4645.

Hernandez RD. **2008**. A flexible forward simulator for populations subject to selection and demography. *Bioinformatics* **24**: 2786–2787.

Hohenlohe PA, Day MD, Amish, SJ, Miller, MR, Kamps-Hughes N, Boyer MC, ... & **Luikart, G**. **2013**. Genomic patterns of introgression in rainbow and westslope cutthroat trout illuminated by overlapping paired-end RAD sequencing. *Molecular ecology **22***: 3002-3013.

~~**Hoffmann AA, Sgró CM. 2011**. Climate change and evolutionary adaptation. *Nature* **470**: 479–485.~~

Huson DH, Bryant D. **2006**. Application of phylogenetic networks in evolutionary studies. *Molecular Biology and Evolution* **23**: 254–267.

Jaramillo-Correa JP, Rodríguez-Quilón I, Grivet D, *et al.* 2015. Molecular proxies for climate maladaptation in a long-lived tree (*Pinus pinaster* Aiton, Pinaceae). *Genetics* **199**: 793–807.

Kawecki T. **2008**. Adaptation to marginal habitats. *Annual Review of Ecology, Evolution, and Systematics* **39**: 321–342.

Kyrkou I, Iriondo JM, García-Fernández A. 2015. A glacial survivor of the alpine Mediterranean region: Phylogenetic and phylogeographic insights into *Silene ciliata* Pourr. (Caryophyllaceae). *PeerJ* **2015**: 1–19.

Lande R. 1994. Risk of population extinction from fixation of new deleterious mutations. *Evolution* **48**: 1460–1469.

Lara-Romero C, García-Fernández A, Robledo-Arnuncio JJ, *et al.* 2016. Individual spatial aggregation correlates with between-population variation in fine-scale genetic structure of *Silene ciliata* (Caryophyllaceae). *Heredity* **116**: 417–423.

Lara-Romero C, Robledo-Arnuncio JJ, García-Fernández A, Iriondo JM. 2014. Assessing intraspecific variation in effective dispersal along an altitudinal gradient: A test in two Mediterranean high-mountain plants. *PLoS ONE* **9**.

Lawlor DW, Cornic G. 2002. Photosynthetic carbon assimilation and associated metabolism in relation to water deficits in higher plants. *Plant, Cell and Environment* **25**: 275–294.

Lenormand T. 2002. Gene flow and the limits to natural selection. *Trends in Ecology and Evolution* **17**: 183–189.

Liu S, Ferchaud AL, Grønkjær P, Nygaard R, Hansen MM. 2018. Genomic parallelism and lack thereof in contrasting systems of three-spined sticklebacks. *Molecular Ecology* **27**: 4725–4743.

López-Moreno JI, Vicente-Serrano SM, Lanjeri S. 2007. Mapping snowpack distribution over large areas using GIS and interpolation techniques. *Climate Research*, **33**: 257.

Lynch M, Gabriel W. 1987. Environmental Tolerance. *The American Naturalist* **129**: 283–303.

Mayol M, Riba M, Cavers S, *et al.* 2020. A multiscale approach to detect selection in nonmodel tree species: Widespread adaptation despite population decline in Taxus baccata L. *Evolutionary Applications* **13**: 143–160.

McKenna A, Hanna M, Banks E, *et al.* 2010. The Genome Analysis Toolkit: A MapReduce framework for analyzing next-generation DNA sequencing data. *Genome Research* **20**: 1297–1303.

McKinney GJ, Waples RK, Seeb LW, Seeb JE. 2017. Paralogs are revealed by proportion of heterozygotes and deviations in read ratios in genotyping-by-sequencing data from natural populations. *Molecular Ecology Resources* **17**: 656–669.

Molau U, Nordenhall U, Eriksen B. 2005. Onset of flowering and climate variability in an alpine landscape: A 10-year study from Swedish Lapland. *American Journal of Botany* **9**: 422–431.

Morente-López J, García C, Lara-Romero C, García-Fernández A, Draper D, Iriondo JM. 2018. Geography and Environment Shape Landscape Genetics of Mediterranean Alpine Species Silene ciliata Poiret. (Caryophyllaceae). *Frontiers in Plant Science* **9**: 1–15.

Morente-López J, Kass J, Lara-Romero C, Serra-Diaz JM, Soto-Correa JC, Anderson RP, Iriondo JM. 2022. Linking ecological niche models and common garden experiments to predict phenotypic differentiation in stressful environments: Assessing the adaptive value of marginal populations in an alpine plant. *Global Change Biology* **28**: 4143-4162.

Morente-López J, Lara-Romero C, García-Fernández A, Rubio Teso ML, Prieto-Benítez S, Iriondo JM. 2021. Gene flow effects on populations inhabiting marginal areas: Origin matters. *Journal of Ecology* **109**: 139–153.

Morente-López J, Scheepens JF, Lara-Romero C, Ruiz-Checa R, Tabarés P, Iriondo JM. 2020. Past selection shaped phenological differentiation among populations at contrasting elevations in a Mediterranean alpine plant. *Environmental and Experimental Botany* **170**: 103894.

~~**Nagasaka K, Nishiyama S, Fujikawa M, *et al.* 2022**. Genome-Wide Identification of Loci Associated With Phenology-Related Traits and Their Adaptive Variations in a Highbush Blueberry Collection. *Frontiers in Plant Science* **12**: 1–18.~~

Nielsen R, Williamson S, Kim Y, Hubisz MJ, Clark AG, Bustamante C. 2005. Genomic scans for selective sweeps using SNP data. *Genome Research* **15**: 1566–1575.

Olson-Manning CF, Wagner MR, Mitchell-Olds T. 2012. Adaptive evolution: Evaluating empirical support for theoretical predictions. *Nature Reviews Genetics* **13**: 867–877.

Opgenoorth L, Vendramin GG, Mao K, Miehe G, Miehe S, Liepelt S, Liu J, Ziegenhagen B. 2010. Tree endurance on the Tibetan Plateau marks the world's highest known tree line of the Last Glacial Maximum. *New Phytologist*, *185*: 332-342.

Pavlidis P, Živković D, Stamatakis A, Alachiotis N. 2013. SweeD: Likelihood-based detection of selective sweeps in thousands of genomes. *Molecular Biology and Evolution* **30**: 2224–2234.

Pickrell JK, Pritchard JK. 2012. Inference of Population Splits and Mixtures from Genome-Wide Allele Frequency Data. *PLoS Genetics* **8**: e1002967.

Pironon S, Papuga G, Villellas J, Angert AL, García MB, Thompson JD. 2017. Geographic variation in genetic and demographic performance: new insights from an old biogeographical paradigm. *Biological Reviews* **92**: 1877–1909.

Pironon S, Villellas J, Morris WF, Doak DF, García MB. 2015. Do geographic , climatic or historical ranges differentiate the performance of central versus peripheral populations ? *Global Ecology and Biogeography* **24**: 611–620.

Pouget M, Youssef S, Migliore J, Juin M, Médail F, Baumel A. 2013. Phylogeography sheds light on the central-marginal hypothesis in a Mediterranean narrow endemic plant. *Annals of Botany* **112**: 1409–1420.

Prieto-Benítez S, Morente-López J, Rubio Teso ML, *et al.* 2021. Evaluating Assisted Gene Flow in Marginal Populations of a High Mountain Species. *Frontiers in Ecology and Evolution* **9**: 1–12.

Pütz J, Jansen S, Reutimann O, Rellstab C, Bordács S, Neophytou C. 2024. The influence of post-glacial migration and hybridization on the gene pool of marginal *Quercus pubescens* populations in Central Europe, *Annals of Botany*, mcae216.

Ramakrishna A, Gill S. 2019. *Metabolic Adaptations in Plants During Abiotic Stress*. Boca Ratón: CRC Press.

Ramírez-Soriano A, Ramos-Onsins SE, Rozas J, Calafell F, Navarro A. 2008. Statistical power analysis of neutrality tests under demographic expansions, contractions and bottlenecks with recombination. *Genetics* **179**: 555–567.

Razgour O, Forester B, Taggart JB, Bekaer, M, Juste J, Ibáñez C, Puechmaille Sj, Novella-Fernandez, RN, Alberdi A, Manel, S. 2019. Considering adaptive genetic variation in climate change vulnerability assessment reduces species range loss projections. *Proceedings of the National Academy of Sciences*, ***116***:10418-10423.

Rull V. 2009. Microrefugia**.** *Journal of Biogeography* **36**: 481-484.

Sacristán-Bajo S, García-Fernández A, Iriondo JM, Lara-Romero C. 2019. Transcriptome assembly and polymorphism detection in *Silene ciliata* (Caryophyllaceae). *Plant Genetic Resources: Characterisation and Utilisation* **17**: 452–455.

~~**Sanz-Elorza M, Dana ED, González A, Sobrino E. 2003**. Changes in the high-mountain vegetation of the central Iberian Peninsula as a probable sign of global warming. *Annals of Botany* **92**: 273–280.~~

Sacristán-Bajo S, Lara-Romero C, García-Fernández A, Prieto-Benítez S, Morente-López J, Rubio Teso ML, Torres E, Iriondo JM,. 2019. Assisted gene flow management to climate change in the annual legume *Lupinus angustifolius* L.: from phenotype to genotype. *Evolutionary Applications* **18**: e70087.

Scheepens JF, Sto J. 2013. Flowering phenology and reproductive fitness along a mountain slope : maladaptive responses to transplantation to a warmer climate in *Campanula thyrsoides*. *Oecologia* **171**: 679–691.

Sedlacek J, Wheeler JA, Cortés AJ, Bossdorf O. 2015. The Response of the Alpine Dwarf Shrub *Salix herbacea* to Altered Snowmelt Timing : Lessons from a Multi-Site Transplant Experiment. *PLoS ONE* **10**: e0122395.

Shaar-moshe L, Hübner S, Peleg Z. 2015. Identification of conserved drought-adaptive genes using a cross-species meta-analysis approach. *BMC Plant Biology* **15**: 111.

Soulé M. 1973. The epistasis cycle: a theory of marginal populations. *Annual review of ecology and systematics* **4**: 165–187.

Stillman Jh, Armstrong E. 2015. Genomics Are Transforming Our Understanding of Responses to Climate Change, *BioScience* **65**: 237–246.

Storey JD, Tibshirani R. 2003, Statistical significance for genome wide studies. *PNAS.* **100**: 9440–9445.

Temunović M, Garnier-Géré P, Morić M, Franjić J, Ivanković M, Bogdan S, Hampe A. 2020. Candidate gene SNP variation in floodplain populations of pedunculate oak (*Quercus robur* L.) near the species' southern range margin: Weak differentiation yet distinct associations with water availability. *Molecular ecology* **29**: 2359-2378.

Theraroz A, Guadaño-Peyrot C, Archambeau J, Pinosio S, Bagnoli, F, Piotti, A, Avanzi C, Vendramin GG, Alía R, Grivet D, Westergren M, González-Martínez SC. 2024. The genetic consequences of population marginality: a case study in maritime pine. *Diversity and Distributions*, **e13910.**

Thompson J. **2020**. *Plant Evolution in the Mediterranean*. Oxford: Oxford University Press.

Thornton KR, Jensen JD. **2007**. Controlling the False-Positive Rate in Multilocus Genome Scans for Selection. *Genetics* **175**: 737–750.

Tintle NL, Borchers B, Brown M, Bekmetjev A. **2009**. Comparing gene set analysis methods on single-nucleotide polymorphism data from Genetic Analysis Workshop 16. *BMC Proceedings* **3**: 1–5.

Vangestel C, Eckert AJ, Wegrzyn JL, St. Clair JB, Neale DB. **2018**. Linking phenotype, genotype and environment to unravel genetic components underlying cold hardiness in coastal Douglas-fir (*Pseudotsuga menziesii* var. *menziesii*). *Tree Genetics and Genomes* **14**.

Vilà-Cabrera A, Premoli AC, Jum AS. 2019. Refining predictions of population decline at species' rear edges. Global Change Biology **25**: 1549–1560.

Yan J, Wang B, Jiang Y, Cheng L, Wu T. **2014**. GmFNSII -Controlled Soybean Flavone Metabolism Responds to Abiotic Stresses and Regulates Plant Salt Tolerance. *Plant and Cell Physiology* **55**: 74–86.

Yang A, Dick CW, Yao X, Huang H. **2016**. Impacts of biogeographic history and marginal population genetics on species range limits: a case study of *Liriodendron chinense*. *Nature Publishing Group*: 1–12.

Yeap WC, Namasivayam P, Ooi TEK, Appleton DR, Kulaveerasingam H, Ho CL. **2019**. EgRBP42 from oil palm enhances adaptation to stress in Arabidopsis through regulation of nucleocytoplasmic transport of stress-responsive mRNAs. *Plant Cell and Environment* **42**: 1657–1673.

Yuan S, Shi Y, Zhou BF, Liang YY, Chen XY, An, QQ, Fan YR, Shen Z, Ingvarsson PK, Wang B. 2023. Genomic vulnerability to climate change in Quercus acutissima, a dominant tree species in East Asian deciduous forests. *Molecular ecology*, **32***:* 1639-1655.

9. LIST OF CAPTIONS

Figure 1. Location of the three main mountain ranges in the Sistema Central of the Iberian Peninsula (Spain) where the study was developed: Bejar (BJR), Gredos (GRD) and Guadarrama (GDM). The three-dimensional coloured map represents an example of the intra-range environmental classification in core (optimal) and marginal areas developed for *S. ciliata* based on ecological niche modelling and putative selective pressures (see Morente-López *et al*. 2022). In each of the three mountain ranges, two populations were selected, one in core (blue) and one in marginal (red) environmental conditions. The approximate locations of the two populations selected in Guadarrama mountain range, Pico de Peñalara (PEN) and Morrena Peñalara (MOR) are depicted in optimal and marginal areas respectively. Black shaded areas in the map represents elevations above 1,500 m. Dashed lines represent political divisions of provinces.

Figure 2. Demographic models tested in Fastsimcoal2. (a) Demographic models tested at population level. Model parameters are bottleneck (T_{BOT}) and expansion (T_{EXP}) times, current (N_{CUR}) and ancestral (N_{ANC}) effective population sizes and population size during the bottleneck event (N_{BOT}). (b) Demographic models tested at mountain range level. Additional model parameters are current population size of marginal (N_M) and core (N_O) populations, time of instantaneous isolation (T_{DIV}) and migration probability from marginal to core (M_{MC}) and core to marginal (M_{CM}) populations (horizontal arrows).

Figure 3. Population genetic structure of *S. ciliata* in the Sistema Central of the Iberian Peninsula (Spain) showing closer relationships between the two western mountain ranges (Gredos and Bejar) and separating the eastern Guadarrama mountain range. Refer to Table 1 for population acronyms. (A) Bayesian cluster analysis (fastStructure). Figure shows the individual bar plot grouped by population and mountain ranges. Bar colours represent individual assignment probability to each of the optimal K=2 groups. (B) Neighbour-net (Nnet) phylogenetic network constructed in SplitsTree v4. (C) Population relationships and migration edges inferred by TREEMIX. Arrows are coloured by migration weight and branch lengths are proportional to genetic drift. Notice that the only migration event linked two populations was found in Bejar and Gredos mountain ranges (NEG-CAM).

Figure 4. Parameters inferred from coalescent simulations with Fastsimcoal2 under the best-supported demographic model for single populations ("Bottleneck" model, see Figure 2a). For each parameter, the point estimate and the lower and upper 95% confidence intervals, generated by parametric bootstrapping, are shown. Model parameters include T_{BOT} (time when the bottleneck ~~time~~began), N_{CUR} and N_{ANC} (current and ancestral population sizes), and N_{BOT} (population size during the bottleneck event).

Figure 5. Parameters inferred from coalescent simulations with Fastsimcoal2 under the best-supported demographic model fitted at mountain range level ("Bottleneck and Isolation of two populations" model, see Figure 2b). For each parameter, the point estimate and the lower and upper 95% confidence intervals, generated by parametric bootstrapping, are shown. Model parameters include: T_{BOT} and T_{DIV} (bottleneck and instantaneous split times), N_M and N_C (current effective population size of marginal and core populations), N_{ANC} (ancestral population size), N_{BOT} (population size during the bottleneck event), and M_{MC} and M_{CM} (migration from marginal to core and core to marginal populations). The red and blue shades visualise the division of the ancestral population into marginal and core populations.

Figure 6. Diagram of the gene pathways tested for signals of selection. Five pathways (indicated with red names) were enriched with positive *alpha* values estimated by BayeScanHierarchical, indicating diversifying selection between populations inhabiting core and marginal environments. The size of the nodes (pathways) is proportional to the number of genes involved. The node colour scale represents the SUMSTAT score. A higher SUMSTAT score indicates stronger signals of polygenic selection within the pathway. Edges represent mutual overlap; nodes are connected if one of the sets has at least three of its genes in common with the other gene set. Edge width is proportional to the number of shared genes. Nodes marked with an asterisk indicate gene pathways that are plant-specific. For clarity, the figure represents only the 51 pathways with a SUMSTAT score higher than the median value of the entire dataset (N=86).

10. TABLES AND FIGURES

Table 1: *Silene ciliata* populations of the Sistema Central (Spain) used in the targeted resequencing experiment. Geographical and environmental characteristics and sample sizes (*N*) for the experiment are also provided.

Population (ID)	Mountain Range	Environment	*N*	Latitude	Longitude	Snowpack	MinT (°C)	Elevation (m)
Canchal Negro (NEG)	BJR	Core	15	40°20′20′′N	5°41′22′′W	0.59	-7.2	2360
Las Cimeras (RUI)	BJR	Marginal	16	40°21′07′′N	5°40′59′′W	0.27	-6.7	2000
Alto del Morezón (ZON)	GRD	Core	15	40°14′57′′N	5°16′08′′W	0.62	-7.7	2380
Los Campanarios (CAM)	GRD	Marginal	16	40°15′42′′N	5°12′55′′W	0.34	-6.0	2000
Pico de Peñalara (PEN)	GDM	Core	17	40°51′02′′N	3°57′24′′W	0.67	-7.8	2400
Morrena Peñalara (MOR)	GDM	Marginal	15	40°50′11′′N	3°57′01′′W	0.33	-5.7	1980

ID, identification of each population; Mountain Range, mountain range of origin: Bejar (BJR), Gredos (GRD) and Guadarrama (GDM); Environment, environmental classification; *N,* sample size; Latitude and Longitude, geographical coordinates; Snowpack, snowpack accumulation values in thaw months~~;~~ range from 0 to 1 (values close to 1 indicate deep snowpack, while values close to 0 indicate null snow cover; López-Moreno *et al.* 2007)); MinT, minimum annual temperature; Elevation, ~~metres~~refers to the mean elevation (in meters above sea level~~.~~) estimated for each population (variation in elevation within populations did not exceed 10 meters).. Geographical and environmental information extracted from Morente-López et al. (2019). Based on Morente-López et al. (2022), the main putative selective pressures for *S. ciliata* are snowpack in the thaw months and ~~minumum~~minimum temperature. These variables were thus crucial to differentiate environmentally marginal and core areas.

30

Table 2. Nucleotide diversity, neutrality tests and inbreeding by population.

Pop/Env	L (bp)	Polymorphic sites		Nucleotide diversity		Neutrality tests			Inbreeding	
		N	%	Tajima's π	Watterson's θ	*TajD*	*FuD*	*FuF*	*F*	Relatedness
NEG/Cor	2,678,634	33,568	47.17	0.00346	0.00338	-0.073	-0.072	-0.077	-0.082	0.056
RUI/Mar	2,684,833	33,747	47.43	0.00337	0.00331	-0.092	-0.134	-0.130	-0.040	0.055
ZON/Cor	2,677,081	34,147	47.99	0.00338	0.00344	-0.231	-0.275	-0.282	-0.044	0.058
CAM/Mar	2,683,788	30,934	43.47	0.00329	0.00303	0.079	0.193	0.173	-0.069	0.053
PEN/Cor	2,679,723	38,336	53.87	0.00346	0.00370	-0.362	-0.471	-0.475	-0.059	0.051
MOR/Mar	2,676,981	34,631	48.67	0.00338	0.00349	-0.263	-0.263	-0.283	-0.041	0.058

TajD, Tajima's *D*; *FuD, Fu & Li's D*; FuF, Fu & Li's F*; F*, average inbreeding coefficient; Relatedness, average pairwise relatedness statistic (unadjusted A_{jk}), with values around zero indicating unrelated individuals.

Table 3. Candidate genes putatively under divergent selection detected in *Silene ciliata*. "Nº SNPs" refers to the number of SNPs detected with Arlequin (ARL) and BayeScanHierarchical approach (BAY). "Category" refers to the group of sequences to which the candidate gene belongs (See section "Selection of genes for sequencing"): A. Response to abiotic stimulus (GO: 0009628); F. Flower development (GO: 0009908); O. Candidate genes related to local adaptation to elevation in previous studies (Sacristán-Bajo *et al.* 2019). "Biological Processes" provides an overview of the main biological processes mediated by the candidate genes.

Gene Id (*S. ciliata*)	Nº SNPs ARL/BAY	Category	Description	Uniprot ID (Best Blast)	Gene ID (Best Blast)	Biological Processes
comp73228	1/1	FO	ATP sulfurylase 1	Q9LIK9	APS1	Hydrogen sulfide biosynthetic process; Response to cytokinin; Response to cadmium ion
m.101530	1/1	A	Oxygen-evolving enhancer protein 1. chloroplastic	P12359	PSBO	Photosystem II assembly and stabilization; response to light intensity, response to water deprivation
m.102611	1/1	FO	Transmembrane protein	Q0WQ99	At4g16850	petal development; positive regulation of cell population proliferation
m.137232	1/1	F	Nuclear-pore anchor	A4GSN8	NUA	Stamen development; Negative regulation of flower development
m.140709	1/1	O	BAG family molecular chaperone regulator 3	Q9LYP4	BAG3	Chaperone-mediated protein folding; positive regulation of cellular process, response to jasmonic acid, response to wounding
m.19977	6/2	FA	Cytochrome P450 71B37	Q9LIP3	CYP71B37	Oxidation-reduction process; response to jasmonic acid, response to wounding, tissue development
m.843	2/2	A	Indole-3-acetic acid-amido synthetase GH3.10	Q9ZNS2	GH3.10	Response to light stimulus
m.87654	1/1	O	Serine carboxypeptidase-like 49	P32826	SCPL49	Proteolysis involved in cellular protein catabolic process
m.8887	1/1	A	Usp domain-containing protein	A5C9Q0	VIT_08s0007g01430	Response to cold; Response to heat; Response to oxidative stress; Chaperone-mediated protein folding

Table 4. Candidate genes with evidence of selective sweeps for *Silene ciliata* in core or marginal populations. "Category" refers to the group of sequences to which the candidate gene belongs (See section "Selection of genes for sequencing"): A. Response to abiotic stimulus (GO: 0009628); F. Flower development (GO: 0009908); O. Candidate genes previously related to local adaptation to elevation in previous studies (Sacristán-Bajo *et al.* 2019).

Gene Id (*S. ciliata*)	Nº Selective sweeps	Category	Env.	Description	Uniprot ID (Best Blast)	Gene ID (Best Blast)	Biological Proccesess
m.133396	1	A	Marginal	Proteasome subunit beta type	Q8LD27	PBF1	Defence response to fungus, incompatible interaction; proteasomal protein catabolic; proteolysis
comp65047	3	A	Marginal Core	Poly(ADP-ribose) glycohydrolase	Q9SKB3	PARG1	Cellular response to DNA damage stimulus; Defence response to fungus; Regulation of DNA repair; Response to osmotic stress, oxidative stress and water deprivation; Rhythmic process; Stomatal closure
comp54123	1	O	Core	Carboxylate clamp type tetratricopeptide repeat protein	F4IRM4	PHOX1	Root hair cell development
comp64011	1	A	Core	DNA mismatch repair	F4JP48	MSH4	Homologous chromosome segregation; Mismatch repair
comp76868	1	F	Core	DNA repair protein	Q9SL02	RAD50	Gametophyte development; Chromosome organization involved in meiotic cell cycle; Telomere maintenance; DNA repair
m.117629	4	OF	Core	Protein TPLATE	F4J8D3	TPLATE	Endocytosis; Pollen development

m.141175	1	O	Core	Uncharacterized protein	A0A0K9RLQ1	SOVF_052510	na
m.28293	1	A	Core	Histone-lysine N-methyltransferase	Q8GZB6	SUVH4	Histone methylation; Maintenance of DNA methylation; Peptidyl-lysine methylation
m.45836	2	O	Core	FAD-binding FR-type domain-containing protein	A0A2P4H4H9	VITISV_024875	Oxidation-reduction process
m.48088	1	A	Core	Sucrose synthase Glycine max	P13708	SS	Nodulation; sucrose metabolic process
m.83703	1	A	Core	ULP_PROTEASE domain-containing protein	A0A0K9S186	SOVF_011010	Proteolysis

35